



Exploring Radium Isotopes as Tracers of Groundwater Inputs and Flushing Rates in Cook Inlet, Alaska

Principal Investigators: Amanda Kelley¹, Will Burt², Josianne Haag¹

¹ College of Fisheries and Ocean Sciences, University of Alaska Fairbanks

² Planetary Technologies, Dartmouth, NS, Canada

October 2022

Final Reports

OCS Study BOEM 2022-045

Contact Information:
uaf-cmi@alaska.edu
<https://www.uaf.edu/cfos/research/cmi>

This study was funded by the U.S. Department of the Interior, Bureau of Ocean Energy Management Alaska OCS Region (Cooperative Agreement M20AC10016) and the University of Alaska Fairbanks. This report, BOEM 2022-045 is available through the Coastal Marine Institute and electronically from <https://www.boem.gov/akpubs>.

The views and conclusions contained in this document are those of the authors and should not be interpreted as representing the opinions or policies of the U.S. Government. Mention of trade names or commercial products does not constitute endorsement by the U.S. Government.

TABLE OF CONTENTS

| | |
|--|-----------|
| List of Tables | iv |
| List of Figures | iv |
| ABSTRACT | v |
| INTRODUCTION | 1 |
| Background..... | 1 |
| Objectives | 3 |
| METHODS | 3 |
| Study Area..... | 3 |
| Constructing radium and nutrient budgets via mass balance (Objective 1)..... | 4 |
| Calculating Offshore mixing rates (Objective 1)..... | 6 |
| Radium-based residence time (Objective 2)..... | 6 |
| Field sampling in Kachemak Bay..... | 7 |
| Collecting and measuring radium isotopes..... | 7 |
| The RaDeCC Isotope Counter | 10 |
| Radium Uncertainties: Logistical Challenges..... | 12 |
| RESULTS | 12 |
| Sampling for Short-lived Radium..... | 12 |
| Constructing Radium and Nutrient Budgets via Mass Balance (Objective 1)..... | 14 |
| Mass-balances across the Jakolof, Grewingk, and Wosnesenski sub-bays | 14 |
| Cross-bay sampling to constrain F_{mix} | 14 |
| Constraining F_{sediment} and F_{rivers} | 16 |
| Groundwater radium endmembers | 18 |
| Nutrient data across Kachemak Bay | 19 |
| Radium mass-balance in Jakolof Bay | 20 |
| Nutrient fluxes in Jakolof Bay | 22 |
| Calculating offshore fluxes..... | 24 |
| Residence Time (Objective 2) | 25 |
| DISCUSSION | 27 |
| Objectives 1 and 2..... | 27 |
| Local Involvement and Scientific Outreach..... | 28 |
| ACKNOWLEDGMENTS | 28 |
| STUDY PRODUCTS | 28 |
| REFERENCES | 29 |

List of Figures

| | |
|--|----|
| Figure 1: Map of the study area..... | 2 |
| Figure 2: Typical radium mass balance for a coastal system..... | 4 |
| Figure 3: Radium extraction methods from seawater, rivers, and groundwater..... | 8 |
| Figure 4: RaDeCC Counter..... | 9 |
| Figure 5: RaDeCC counting schematic..... | 11 |
| Figure 6: Results of efficiency testing..... | 12 |
| Figure 7: Radium surveys as planned and carried out in the fall, spring, and summer..... | 13 |
| Figure 8: Radium activities and temperature and salinity across the Homer spit transect during fall 2020..... | 15 |
| Figure 9: Spring and summer radium data across the Homer spit transect..... | 15 |
| Figure 10: Vertical radium profile from Jakolof Bay station J4..... | 16 |
| Figure 11: Photo of salting experiment samples on the Grewingk River bank and graph showing experiment results..... | 18 |
| Figure 12: Relationship between groundwater radium and salinity in the Jakolof Bay wells..... | 19 |
| Figure 13: Jakolof Bay sampling stations..... | 20 |
| Figure 14: Radium-224 measured along Kachemak Bay transect during fall 2020..... | 25 |
| Figure 15: Activities of radium-224, radium-226, and radium-228 along the Jakolof Bay sampling transect for all three seasons..... | 26 |

List of Tables

| | |
|--|----|
| Table 1: Extraction efficiencies of radium from seawater under varying flow rates and radium activities..... | 9 |
| Table 2: Riverine radium-224 activities measured across Kachemak Bay..... | 17 |
| Table 3: Radium mass balance terms, and resulting SGD calculation..... | 20 |
| Table 4: The concentration of nutrients in the river and groundwater across seasons in Jakolof Bay..... | 22 |
| Table 5: Nitrate, phosphate, and silicic acid fluxes from the Jakolof river (riverine) and the Jakolof mudflats (groundwater) across fall, spring, and summer seasons..... | 23 |

ABSTRACT

This project presents novel and innovative methods for tracing the flow of seawater and its dissolved constituents into, through, and out of Kachemak Bay. Oceanographic surveys in Kachemak Bay collected radium isotope samples to assess the feasibility of creating radium budgets to characterize groundwater inputs, a potentially dominant source of freshwater, carbon, and nutrients to the Gulf of Alaska. Creating radium budgets throughout Kachemak Bay was too challenging for the scope of this project but was accomplished for Jakolof Bay, a small sub-bay with favorable basin geometry. Results show that groundwater contribution of nitrate and silicic acid to Jakolof Bay is comparable to or larger than river sources, that groundwater nitrate plays an important role in buffering nitrate limitation during summer, and that tidal pumping into groundwater may act as a sink for phosphate. We tested the feasibility of isotope ratio analyses to yield estimates of water residence time, a vital piece of information that remains unquantified in current oil spill risk analyses and environmental impact statements for Cook Inlet. The natural abundance of short-lived radium in this area is very low, leading to challenges in collecting and analyzing samples for radium-223. Instead, we analyzed a select group of samples for long-lived radium (radium-228 and radium-226). Results indicated that the offshore waters that enter Kachemak Bay from the Northern Gulf of Alaska are relatively enriched in long-lived radium, which violates a key assumption needed to perform the residence time calculations. Surface radium transects were used to estimate rates of cross-shelf mixing, which can inform about how rapidly dissolved materials and pollutants can disperse from Cook Inlet into the Gulf of Alaska, which contains many of the largest and most valuable fisheries in the nation.

INTRODUCTION

Background

Given the current scope of oil and gas exploration and development activities in Cook Inlet, it is important to develop tools and methods to trace the flow of water and its dissolved constituents into, through, and out of the region. For example, nutrient inputs into coastal areas, like those across the Cook Inlet region, can fuel primary productivity which sustains the growth of marine species vital to local subsistence harvests, growing aquaculture industries, and marine tourism. However, it remains unclear whether the primary source of nutrients to these areas is the marine environment (i.e., advected in from the Alaska Coastal Current) or localized inputs from seafloor sediments and land-based sources (i.e., rivers and groundwater). While some data are available regarding river inputs (e.g., Brabets et al., 1999), little information exists regarding inputs from groundwater and the seafloor, two relatively inaccessible but often important nutrient reservoirs (Burt et al., 2013a; 2013b; 2014; 2016).

In fact, in many coastal systems, groundwater nutrient fluxes outweigh riverine sources (Santos et al., 2009; Knee and Paytan, 2011). Globally, groundwater fluxes to the ocean are three to four times greater than freshwater fluxes from rivers and are a dominant pathway for dissolved terrestrial materials to enter our seas (Kwon et al., 2014). This flux of water across the seabed is termed submarine groundwater discharge (SGD). In 2011, a study in Kasitsna Bay highlighted that SGD nutrient fluxes may outweigh river fluxes, and a follow-up study showed that SGD can spark large diatom blooms in the bay (Lecher et al., 2016; 2017). Tidal pumping is often a dominant mechanism of SGD, whereby seawater injected into permeable sediments during the flood tide mixes with sediment porewaters enriched in dissolved solutes before being drawn back into the water column during the ebb tide (Burnett and Dulaiova, 2003; Liu et al., 2017). However, SGD studies in areas with extreme tidal ranges are lacking.

A considerable amount of Cook Inlet (Figure 1) is underlain by soft permeable sediment (Oey et al., 2007), and the inlet's tidal range is among the largest on the planet (Archer, 2013). These factors suggest the potential for enormous SGD, which could play a key role in local biogeochemical cycles. Dozens of bays across southern Alaska have seafloor sediment and tidal forcing analogous to Kachemak Bay and Cook Inlet. Groundwater could be critical to nutrient budgets throughout the Northern Gulf of Alaska region. River and groundwater inputs are likely to play an increasingly important role in sub-arctic systems due to accelerating glacial and permafrost melt. With active oil industry activity in place in some areas of Cook Inlet and rapid environmental change underway, it is important to establish a baseline understanding of the dominant drivers of nutrient and carbon cycles in these areas.

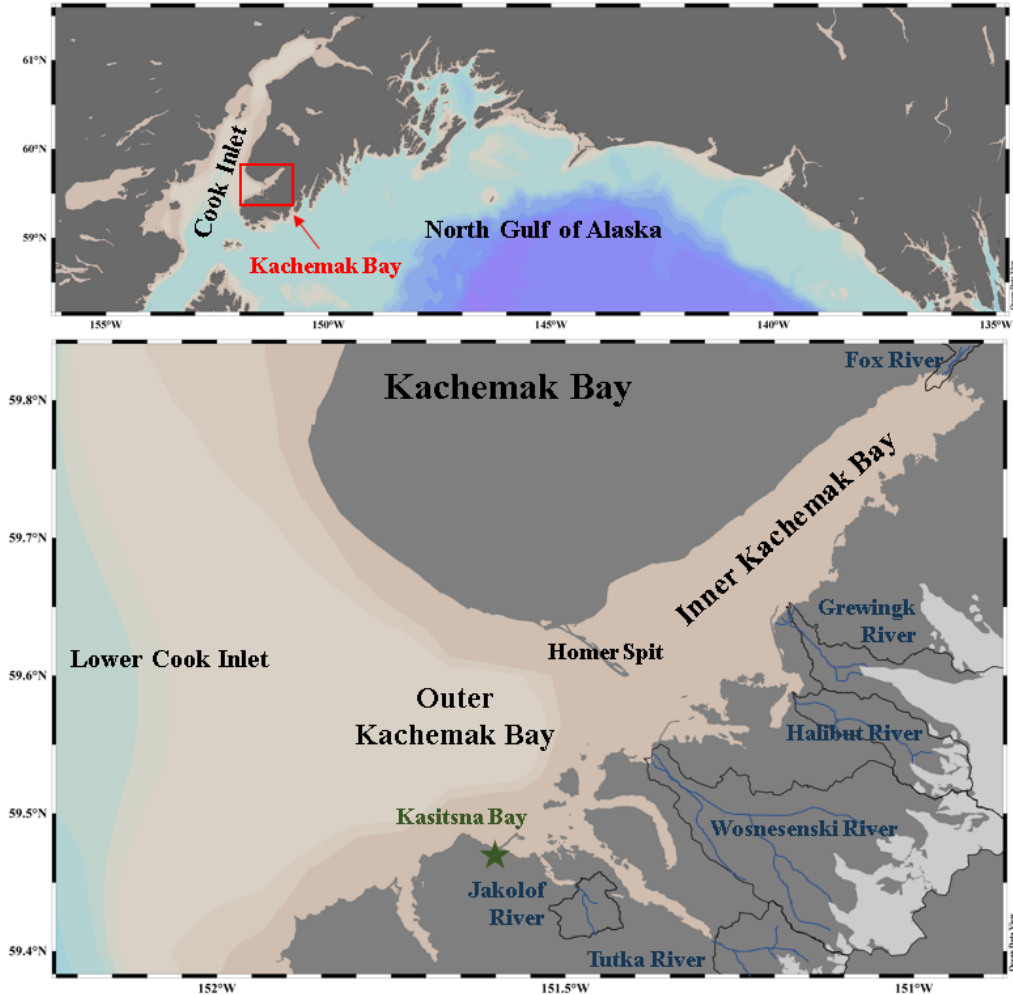


Figure 1: Map of the study area. (top) Kachemak Bay within the greater Northern Gulf of Alaska and (bottom) the Cook Inlet region showing the locations of the six rivers (blue) relevant to this study and their respective watersheds (black).

Identifying rates at which nutrient-enriched waters are flushed through and out of Cook Inlet is a key to understanding nutrient availability. Over four decades ago, a surface drifter study in outer Cook Inlet yielded a residence time of approximately 15 days (Burbank, 1977). This represents the only peer-reviewed study of residence time in Cook Inlet. In Kachemak Bay, Gatto (1976) used a ‘prism method’, the sum of low and intertidal volumes divided by the intertidal volume, to estimate flushing times ranging from 3 to 32 days depending on seasonal runoff. An unpublished satellite drifter study estimated flushing times ranging from 8 to 19 days (Kachemak Bay National Estuarine Research Reserve Quarterly Report, February 2017). Comprehensive work is needed to develop accurate residence time estimates and to understand how residence times vary both spatially and seasonally.

Naturally occurring radium isotopes are well established as ideal water mass tracers in coastal systems. Radium enters the marine water column at the land-ocean and sediment-water column interfaces, so it is commonly used to trace groundwater and benthic discharges into the

water column. Four radium isotopes are present in marine systems, two short-lived species (radium-223 and radium-224; 3.66-day and 11.43-day half-lives, respectively) and two long-lived species (radium-228 and radium-226; 5.75-year and 1600-year half-lives, respectively). This radium ‘quartet’ can be used to trace marine processes across a wide range of temporal scales. The use of multiple isotopes facilitates the measurement of isotope ratios, which are commonly applied to estimate water residence times in coastal systems (Dulaiova and Burnett, 2008; Santos et al., 2009, and others).

The results of this project provide a baseline understanding of the naturally occurring radium isotope activities in Kachemak Bay, give insights into the key radium sources, and test the feasibility of two radium-based approaches that have useful applications related to ecosystem health.

Objectives

The project objectives and associated hypotheses are as follows:

Objective 1: Construct radium and nutrient mass balance for Kachemak Bay using data from a comprehensive field survey and assess the relative importance of different land-based sources (rivers, groundwater, seafloor) as well as the marine input (from outside the bay) to regional nutrient cycles. Key hypotheses under this objective include:

Hypothesis 1a. Localized nutrient fluxes from within Kachemak Bay outweigh the marine source, and more specifically, groundwater inputs driven by strong tidal pumping outweigh both riverine and seafloor sources.

Hypothesis 1b. Results from Kachemak Bay suggest offshore nutrient export as an important source term for nutrient budgets in the Gulf of Alaska.

Objective 2: Estimate water residence times in Kachemak Bay using radium isotope ratios and compare and contrast results to those from the ongoing drifter-based study. Key hypotheses under this objective include:

Hypothesis: Residence times are on the order of two to four weeks, and compare well with drifter-based results.

METHODS

Study Area

Kachemak Bay is located in the Cook Inlet region of southcentral Alaska (Figure 1). Multiple large rivers enter Kachemak Bay along its southern coast. These rivers drain watersheds with varying degrees of glacial cover, so their chemical composition and seasonal discharge patterns vary considerably. Kachemak Bay exhibits high biological productivity in the summer months and has been considered among the planet’s most diverse estuaries (Konar et al., 2010).

Kachemak Bay connects to lower Cook Inlet through a channel south of Homer Spit (Figure 1). Some Gulf of Alaska water entering lower Cook Inlet mixes with water in outer Kachemak Bay and circulates counter-clockwise through the inner bay, exiting in a narrow fast-

moving current at the northern side of the channel (Gatto, 1976; Burbank 1977; Johnson, 2021). We surmised that we could measure the radium activity immediately inside and outside of Kachemak Bay by sampling a transect between Homer Spit and the southern coast of Kachemak Bay. This information could be used to constrain the F_{mix} term of the mass balance (see equation outlined in the Method section). This transect was completed in all three seasons.

Jakolof Bay, located along the southwestern coastline of outer Kachemak Bay, was used as a test site before scaling up to Kachemak Bay (Figure 1). Jakolof Bay has an extensive mudflat at its head and minimal river discharge. The heavily forested watershed feeding into the Jakolof River is not glaciated; therefore, the river can dry out in summer after spring snowmelt and heavy rainfall have stopped. As the river discharge decreases into late summer, terrestrial nutrient input should primarily be derived from SGD. The rate of SGD could be substantial in Jakolof Bay, due to high mean annual precipitation (450 to 800 mm), high topographical relief, and large tidal ranges (over 8 m). However, SGD may be constricted to areas of coarser sand due to the impermeable mud within the bay.

Constructing Radium and Nutrient Budgets via Mass Balance (Objective 1)

Mass-balance is a common approach to calculating key fluxes in physical systems (carbon, nutrients, radium, or other dissolved material). A mass balance is a single equation that balances all sources and sinks for a specific parameter (assumes a steady state, i.e., sources = sinks). Characterizing point sources (i.e., rivers, advection into the bay) is straightforward, but it is very difficult to accurately quantify fluxes due to biological interactions or widespread diffusive sources (i.e., groundwater). However, radium has well-defined sources and undergoes no biological or atmospheric interactions, greatly simplifying the mass balance by allowing isolation of a specific source term. Consequently, the radium mass balance approach has been used to isolate numerous key fluxes in coastal systems (e.g., Moore et al., 2011; Burt et al., 2013a, 2016). The typical sources and sinks of radium into a coastal system are illustrated in Figure 2.

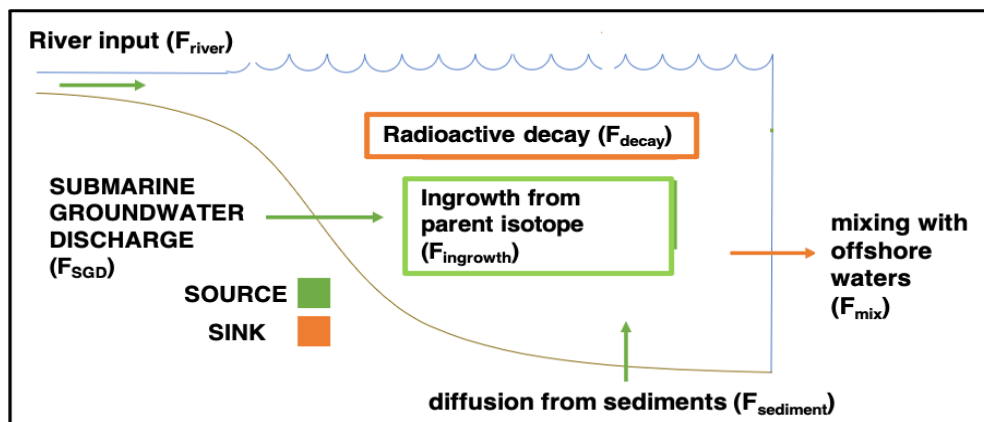


Figure 2: Typical radium mass balance for a coastal system.

Solving the mass balance for the submarine groundwater discharge term (F_{SGD}) can be described as:

$$F_{gw} = F_{river} + F_{sediments} + F_{ingrowth} - F_{mix} - F_{decay}. \quad (\text{Eq. 1})$$

The river flux (F_{river}) was calculated by multiplying the riverine radium activity by the river discharge (see Jenckes et al., 2022). Radium loss due to decay (F_{decay}) was calculated by multiplying the average radium activity within the bay by the given isotope's decay constant. Flux from sediments ($F_{sediments}$) was calculated during the following laboratory experiment (no replicates):

Approximately 300 g of sediments were hand-collected from the Jakolof Bay mudflat (GPS coordinates: 59.4504, -151.4875), stored in a Ziploc, frozen, and transported to the University of Alaska Fairbanks (UAF). Sediments were then placed in a bucket and allowed to equilibrate with radium-free water. Sediment thickness in the beaker exceeded 20 cm. After 1 week, the overlying water was removed and measured on the radium counter (see below for counting details). Any radium found in the overlying water is assumed to be derived from the diffusive flux from sediments ($F_{sediment}$). Radium also enters the water column via decay from its parent isotope ($F_{ingrowth}$). For radium-224, the parent isotope (radium-228) has a sufficiently long half-life (i.e., decays sufficiently slowly) to assume this ingrowth term is negligible. Radium is lost from the coastal system by mixing with offshore waters (F_{mix} , typically a radium sink because short-lived radium activities are lower offshore). F_{mix} is calculated using the following equation:

$$F_{mix} = \frac{V_{bay}}{\tau} (Ra_{bay} - Ra_{offshore}) \quad (\text{Eq. 2})$$

Where τ is the residence time, V_{bay} is the volume of the bay, Ra_{bay} is the average radium activity in the bay, and $Ra_{offshore}$ is the average radium activity in offshore waters. Given residence times could not be calculated via radium-based methods, we employed a tidal prism approach, where we split the bay into 40 slices along its length and calculated the volume of each one, assuming that they are approximately a triangular prism (Wang et al., 2015), by using satellite imagery of the bay and smoothed bathymetry from our transects. The difference in bay volume at high tide and low tide allowed for the tidal prism to be calculated. The tidal heights were as follows: 9 September 2020 (fall) high tide was 5.6 m and low tide was 0.185 m, 13 May 2021 (spring) high tide was 5.385 m and low tide was 0.225 m, and 11 July 2022 (summer) high tide was 5.41 m and low tide was 0.17 m.

To quantify all these terms, we proposed to focus sampling in three ways: (1) sample throughout Kachemak Bay and Jakolof Bay to determine average radium and parent thorium activities, which were then used to quantify F_{decay} and $F_{ingrowth}$, (2) sample inside and outside Kachemak Bay and Jakolof Bay to determine the mixing loss term (F_{mix}), and (3) sample riverine, sediment, and groundwater endmembers to determine F_{river} , $F_{sediment}$, and F_{gw} respectively.

In this study, we hypothesized that the primary radium sources in both bays would be rivers and groundwater, both of which are functions of discharge and the radium concentrations

measured within the rivers or groundwater (referred to as ‘endmember’ concentrations). Thus, we aimed to accurately constrain riverine and groundwater endmembers, along with all other sources and sinks (as described above), to solve for equation (1) and subsequently calculate groundwater discharge rates:

$$F_{gw} = \text{discharge}_{\text{groundwater}} \times [\text{Ra}]_{\text{groundwater}} \rightarrow \text{discharge}_{\text{groundwater}} = \frac{F_{gw}}{[\text{Ra}]_{\text{groundwater}}} \quad (\text{Eq. 3})$$

Similarly, then, multiplying $\text{discharge}_{\text{groundwater}}$ by other endmember concentrations (i.e. nutrients) yields groundwater fluxes. These values can then be directly compared to other key sources of nutrients (i.e., inputs from rivers and offshore waters).

Calculating Offshore Mixing Rates (Objective 1)

The second hypothesis of Objective 1 utilizes a method outlined by Moore (2000b) whereby offshore radium transects are used to calculate rates at which materials are exported from the shallow shelf into the open ocean. Briefly, the decline in radium concentration is used to calculate a horizontal mixing coefficient (K_X), which is then multiplied by horizontal concentration gradients of any solute (e.g., carbon, nutrient, contaminant) to yield a flux using Ficks Law ($Flux = K_X \times dC/dz$). This method has been applied in many systems (e.g., Burt et al., 2013a; 2013b).

To test this method in Kachemak Bay, samples were collected along a transect beginning in the inner bay and extending offshore. Radium activity was plotted with distance offshore, and following the Moore (2000b) method, the natural logarithm of radium activity (i.e., $\ln(\text{Ra}-224)$) is plotted against distance, with the slope of the linear regression (m) used to estimate K_X following the formula:

$$K_X = \frac{\lambda}{m^2} \quad (\text{Eq. 4})$$

Where λ is the decay constant for radium-224 (0.191 day^{-1}). Gradients in nutrients and/or carbon (if present) were then multiplied by K_X to yield an offshore flux.

Radium-based Residence Time (Objective 2)

The natural presence of multiple radium isotopes with varying decay rates facilitates the calculation of ‘apparent water ages.’ If radium is added to a system at a specific ratio (say, Radium-224/Radium-223) then changes in that ratio should only be a function of decay. Therefore, if the isotopic ratio of the dominant radium source (expected to be groundwater) can be measured accurately, then one can calculate water residence time. This method was developed by Moore (2000a) and has been used in a wide range of coastal systems (Dulaiova and Burnett, 2008; Rapaglia et al., 2010; Gu et al., 2012,). Here, we chose to measure the ratio of Radium-224 to Radium-223 ($^{224}\text{Ra}/^{223}\text{Ra}$) for two reasons: (1) the RaDeCC counter purchased for this work measures these two isotopes with strong accuracy and precision, and (2) based on prior work (e.g., Dulaiova and Burnett, 2008), the residence time is expected to be on the order of days-to-weeks. In theory, water will move away from a given source and age, during which time ^{224}Ra decays faster than ^{223}Ra , and apparent radium ages of the water can be estimated by:

$$\left[\frac{Ra^{224}}{Ra^{223}}\right]_{obs} = \left[\frac{Ra^{224}}{Ra^{223}}\right]_{initial} * \left[\frac{e^{-\lambda_{224}t}}{e^{-\lambda_{223}t}}\right] \quad (\text{Eq. 5})$$

Where *obs* and *initial* reference the observed ratio at a given location and the constant endmember ratio of the single source, respectively. The equation is solved for *t*, the apparent radium age.

This approach requires three key assumptions: (1) radium enters the system from a single dominant source, (2) the isotopic ratio of that source remains constant over the timeframe of ~1 week (the effective mean life of the ²²⁴Ra/²²³Ra activity ratio), and (3) as waters mix away from the source, they are diluted by waters with little-to-no excess radium (in other words, the offshore water is depleted in radium).

Field Sampling in Kachemak Bay

We conducted field campaigns in Kachemak Bay that spanned three seasons: fall (21–25 September 2020), spring (12–22 May 2021), and summer (10–18 July 2021). Fieldwork was conducted out of the NOAA-based Kasitsna Bay Laboratory. Seawater samples were collected from a Munson boat that provided adequate deck space to collect up to six radium samples at one time. Across the three field surveys, we collected 107 large-volume samples for radium-223 and radium-224 from 47 ocean sites and 6 river sites. Radium sampling was accompanied by surface measurements of seawater temperature and salinity (taken using a YSI probe), and vertical profiles of temperature and salinity were made using a conductivity/temperature/depth profiler (RBR Concerto CTD). We collected 97 nutrient water samples, filtered them through a 0.49 μm filter, and stored them in acid-cleaned HDPE bottles for analysis at the UAF. Nutrient analysis was done by the Aguilar-Islas group at UAF using a Seal Analytical continuous-flow QuAAtro39 AutoAnalyzer (Murphy and Riley, 1962; Armstrong et al., 1967; Kerouel and Aminot, 1997) for nitrate, ammonium, phosphate, and silicic acid. Radium sample collection and analysis are detailed in subsequent sections.

The fall 2020 campaign focused on testing methods and logistics and gaining a baseline understanding of radium activities around the area. The fall 2020 survey represented the first radium survey in the study area and the first fieldwork of any kind for our laboratory group. The scope and success of subsequent surveys relied heavily on the results from the fall campaign.

Collecting and Measuring Radium Isotopes

Radium isotopes were collected from seawater, rivers, and groundwater. Except for one vertical profile (collected using a bilge pump connected to a long piece of tubing), all seawater radium samples were collected using the vessel's seawater intake system (approximately 0.5 m depth). Due to the low activities of radium in the ocean, large volumes of water must be collected per sample. To obtain reliable activity estimates in the laboratory, we obtained samples of greater than 100 L to get high count rates with respect to background counts (Moore 2008). Sample volumes were estimated using volume level demarcations on the large sample containers (garbage cans or HDPE plastic drums). River samples were collected from six rivers: Jakolof, Tutka, Wosnesenski, Halibut, Grewingk, and Fox rivers (Figure 1).

Accurately constraining the riverine radium flux represented a critical piece of our proposed mass balance, so we tested the adsorbed radium hypothesis by conducting a ‘river salting experiment’ during the spring survey. Five 100-liter samples were collected at Grewingk River. One sample was held as an untreated reference, and four samples were spiked with table salt NaCl: 500g (salinity 5), 1000g (salinity 10), 1500g (salinity 15), and 2000g (salinity 20).

Groundwater was collected using constructed 5-foot PVC pipe wells (Figure 3). Small holes were drilled through the bottom foot of the PVC pipe, which was then covered with fine mesh. Within the intertidal zone, the wells were placed in holes (~2 ft deep), with the space around the bottom foot of the well filled with gravel to create larger interstitial spaces for groundwater to flow. The hole was then topped with the removed sediment. The wells were left for at least two tidal cycles to ensure adequate flushing of the well and return to more natural conditions in the disturbed aquifer. The 2-inch PVC used for the wells was wide enough to fit a HOBO logger to track the salinity and temperature of the surface aquifer over multiple tidal cycles. Ra was collected by dropping a submersible pump into the well (Figure 3). In spring 2021 in Jakolof Bay, the wells were deployed in a ‘T’ formation with the following GPS coordinates: (59.4500, -151.4856), (59.4501, -151.4860), (59.4502, -151.4867), (59.4500, -151.4861), and (59.4498, -151.4862). In summer, two groundwater samples were taken: one from the north side of Kachemak Bay (59.6385, -151.4800), and one from the south side of Kachemak Bay (59.4502, -151.4861).

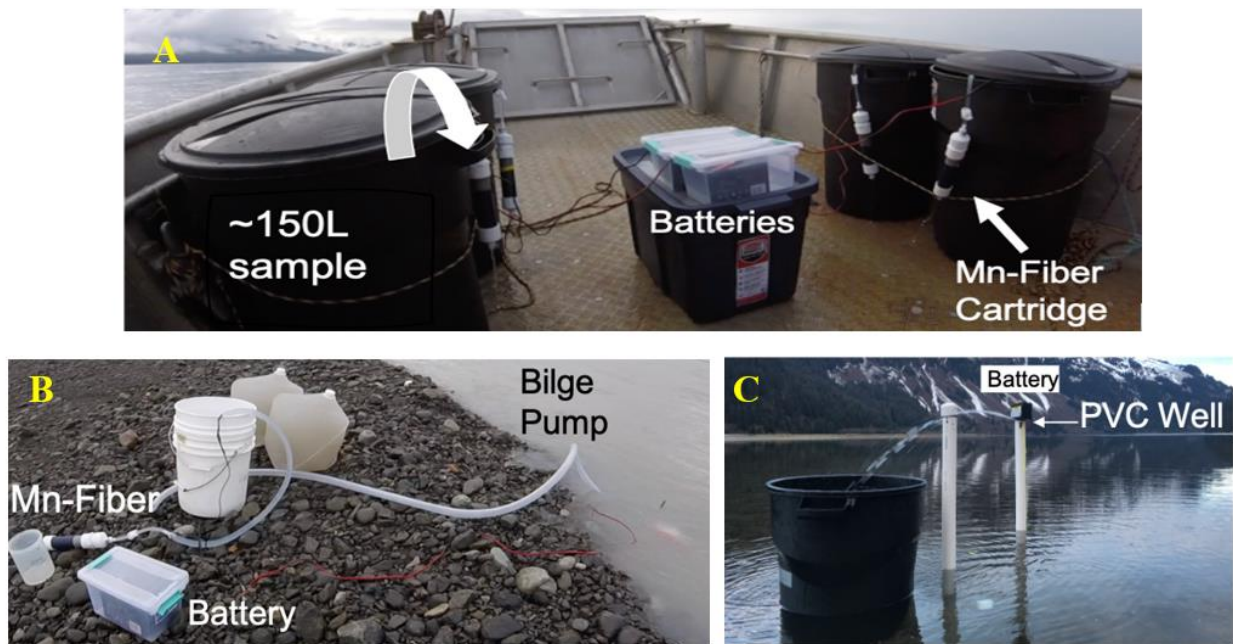


Figure 3: Field sampling photos: (A) Radium extraction from four large-volume seawater samples while onboard the Munson boat operated by the Kasitsna Bay Laboratory. Water is pumped out of the garbage cans and through a plastic cartridge packed with manganese oxide-impregnated (MnO_2) fiber before spilling onto the boat deck. (B) River samples were collected by placing bilge pumps directly into streams. (C) Groundwater sample being collected from a PVC well in Jakolof Bay.

Radium was extracted from the large-volume samples by pumping the water through a plastic cartridge filled with 25g of acrylic fiber coated in manganese oxide (MnO_2). This was achieved by submersing a small bilge pump into the sample container and powering the pump using small 12V batteries. This extraction setup, shown in Figure 4, was developed in-house with assistance from colleagues at the University of California Santa Cruz. MnO_2 was used because it has a large binding surface that can scavenge dissolved metals from the seawater, including radium, lead, mercury, copper, zinc, cobalt, and cadmium (Moore 1976). The water was pumped through the fiber at a rate of < 2 L/min to maximize the efficiency of radium extraction.

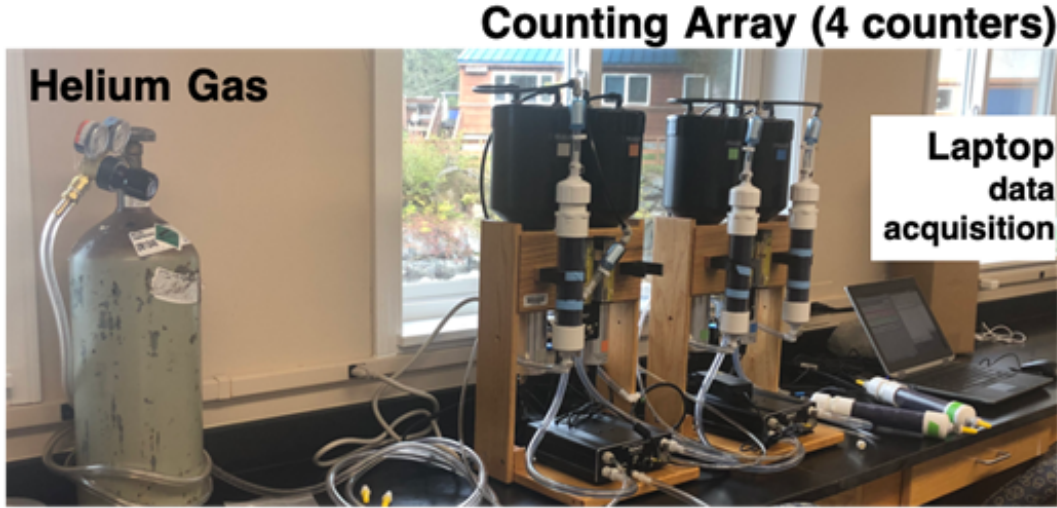


Figure 4: RaDeCC isotope counter set up at the Kasitsna Bay Laboratory in Fall 2020. The image shows three background samples running, with counter #2 sitting empty during a flushing cycle.

The extraction efficiency (E_{ext}) of the MnO_2 fibers were quantified by putting two cartridges in series and measuring the radium activity on the first fiber (A) and the second fiber (B):

$$E_{ext} = \frac{A}{A+B} \times 100\% \quad (\text{Eq. 6})$$

In the fall of 2020, three efficiencies were run using radium-224. These results are summarized in Table 1.

Table 1: Extraction efficiencies of radium from three separate seawater samples under varying flow rates (L/min) and radium activities (dpm).

| ^{224}Ra Activity (dpm/100L) | Filter Rate (L/min) | Extraction Efficiency (%) |
|---------------------------------------|---------------------|---------------------------|
| 0.28 | 1.81 | 92.5 |
| 1.06 | 1.4 | 89.0 |
| 2.72 | 1.4 | 86.3 |

Following extraction, the MnO₂ fibers were rinsed with deionized (DI) water to remove salt crystals. The presence of salt crystals during the activity counts in the laboratory will decrease the instrument efficiency by inhibiting radon emanation from the fibers (Sun and Torgersen, 1998). MnO₂ fibers were then wrung out by hand and repeatedly weighed until reaching a water: fiber ratio of 0.3–1.1 (in other words, until the wet fiber weighed less than 52g, following Moore, 2008). After drying, the MnO₂ fibers are placed back in their cartridges and counted on the RaDeCC isotope counter as quickly as possible. The importance of counting samples quickly is detailed below.

The RaDeCC Isotope Counter

The Radium Delayed Coincidence Counter (RaDeCC) is used to measure activities of radium-223 (half-life 11.43 days) and radium-224 (half-life 3.66 days) on MnO₂ fibers. The RaDeCC consists of four independent counters that can work simultaneously. The radioactivity they measure refers to the number of decays that occurs per unit of time.

A sample cartridge is mounted on the RaDeCC system and the MnO₂ fiber emanates the gaseous radon daughter isotope. To optimize the radon emanation efficiency, the MnO₂ fibers are wetted to a ratio of 0.3–1 gram of water to a gram of fiber. If the fiber is too wet, radon escape will be inhibited, but if the fiber is too dry, the recoiling radon atoms will become embedded in adjacent MnO₂ fiber particles. Counters are flushed with ambient air between samples to dry out any moisture in the tubing and lower any background levels in the counter. Before counting each sample, a background measurement was taken for a minimum of 30 minutes. If counts registered were higher than threshold background values (2, 0.05, and 0.05 counts per minute, see Moore et al. 2008), the sample run was aborted and the counter was left to flush for a longer period.

Helium gas, which strips the radon daughter isotopes from radium, is used because (a) its low density allows alpha particles to travel a longer distance in the scintillation cell (counting cell) and (b) its differing density to ambient air can detect leaks in the closed loop by looking at the flow meter. The airflow is regulated to get the residence time of the gas in the closed loop to 24.6 seconds (airflow is 6 L/min, helium flow is 3.4 L/min). This gas residence time allows the radon-222/polonium-216 and radon-219/polonium-215 pairs to mostly decay in the counting cell.

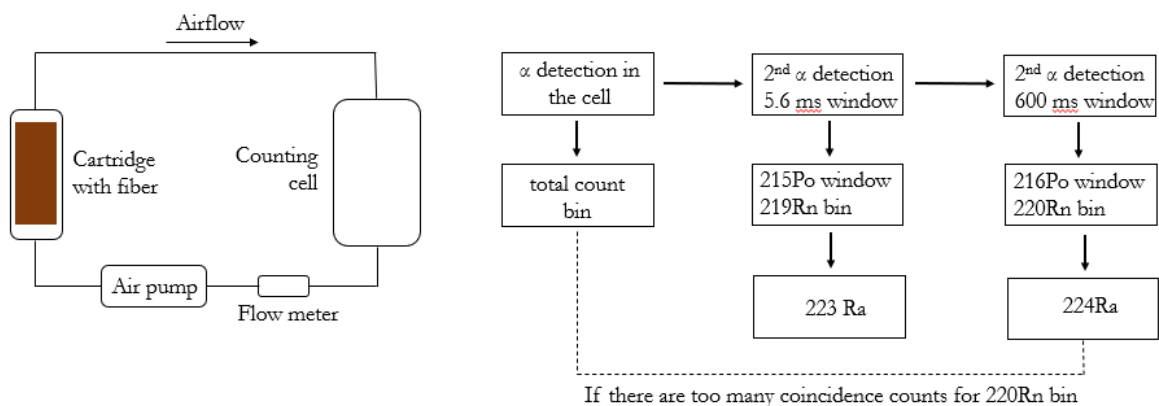


Figure 5: A schematic showing the RaDeCC system layout and a flowchart showing how the counts are allocated to the bins. Adapted from Moore and Arnold (1996).

The counts measured on the RaDeCC, recorded as counts per minute (cpm), were converted to isotopic activity using a series of stepwise equations. Briefly, a series of corrections are applied to radium measurements to account for spurious decay counts, counter efficiency, decay from the time of sampling, and ingrowth of other isotopes, with each correction having an associated error calculation that is propagated through the procedure. Uncertainties for the short-lived radium isotope data can vary considerably and are larger in offshore waters where the radium signal is near background levels. See Garcia-Solsona et al. (2008) for a detailed description of these processing and uncertainty propagation equations. The resulting activity is reported as decays per minute per liter of water (dpm/L).

Accurate radium measurements require the use of standard reference materials ('standards'). The standards are MnO₂ fibers with known activities of radium-223 and radium-224 that are run before, during, and after counting samples. Standard fibers were acquired from the University of Rhode Island before each sampling campaign. Additionally, in spring 2021 we acquired the 'gold-standard' inter-calibration fibers from Woods Hole Oceanographic Institute to further calibrate our system. The ratio of the activity measured by our RaDeCC system to the known activity on a standard fiber is defined as the system efficiency. This value, along with its associated uncertainty, was applied during the data processing steps.

Overall, system efficiencies were relatively stable (Figure 6), with mean values during sampling campaigns ranging from 51–60 %. The instrument appeared more stable in the UAF laboratory than in the field (Kasitsna Bay Lab), which is somewhat typical for many chemical analyses. The counters also appeared more stable in 2021 compared to 2020, which could be due to seasonality or because the 2020 samples were the first analyzed on the new instrument. Further analysis of efficiencies was done using a factorial ANOVA. There were no significant interaction terms, but location (laboratory vs. field) and year were significant factors for system efficiency ($p=0.035$ and $p=0.042$, respectively).

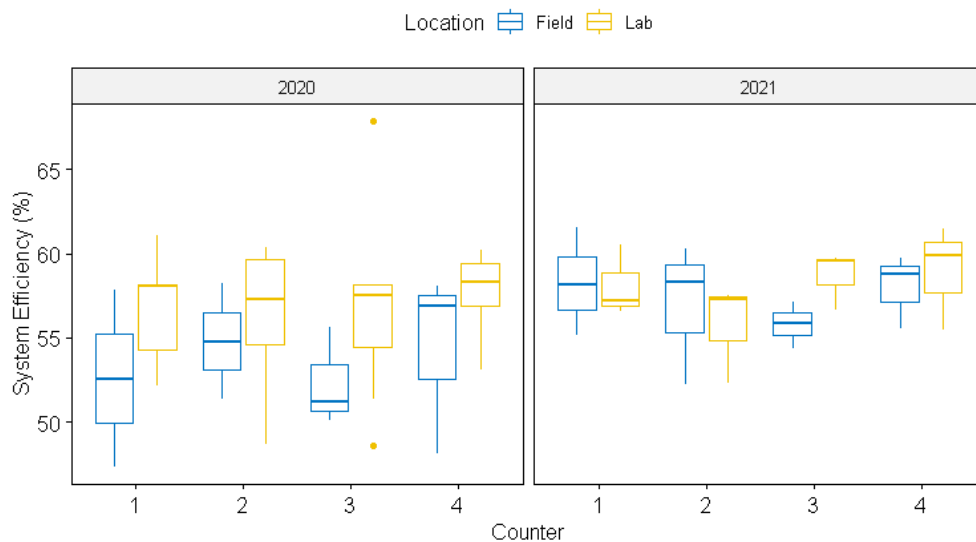


Figure 6: A boxplot showing the results of an ANOVA that indicates that the year and counter location affected the system efficiency.

Radium Uncertainties: Logistical Challenges

Raw analytical uncertainties for radium-224 and radium-223 measurements are directly related to the number of counts registered while counting a sample, with additional uncertainties propagated during data processing (e.g., instrument efficiency). For example, a sample counted long enough on the RaDeCC to register 400 counts has a counting uncertainty of 5%. Radium activities in a sample are constantly decreasing as the sample decays, presenting a critical logistical challenge: counting each sample long enough to achieve low uncertainties without allowing subsequent samples to decay considerably while waiting to be counted. To avoid creating a backlog, a limited number of samples can be taken on a given day. These limits are largely determined by the natural radium activities in the sampling environment, which was largely unknown in the Kachemak Bay/Cook Inlet region prior to this study. To set clear and consistent sample counting procedures, we aimed to count each sample until 400 counts were registered in the radon-220 channel, which would yield a raw analytical radium-224 uncertainty of 5%.

RESULTS

Sampling for Short-lived Radium

The goal of this project was to assess the utility of radium isotope tracers in the Cook Inlet region. Therefore, the first step was to evaluate sampling success and resulting data quality for short-lived radium (radium-224 and radium-223). This began with purchasing, building, and calibrating the RaDeCC isotope counter. Results of instrument calibration are described in the previous section.

The large-volume radium-223 and radium-224 samples collected across all three field surveys are displayed in Figure 7. The majority of these were surface seawater samples, where radium-224 activities ranged from 0.3–7.5 dpm/100L (mean activity = 3.18 dpm/100L). The lowest values were found in outer Kachemak Bay. The highest values were measured in spring and summer along the northern coast of the inner bay. Sample volumes were made as large as possible,

ranging from 5.78–209 L and averaging 141 L. Although activities were generally lower than anticipated, the large sample volumes and our sample counting protocol (a 400-count threshold, see above) led to reasonable and relatively stable radium-224 uncertainties, ranging from 4–61 % with an average of 8.32%. In fall 2020, a triplicate radium sample was taken near the Homer Spit (sample T10: 3.86, 3.42, and 3.56 dpm/100L), and a duplicate sample was taken at the Wosnesenski River (sample Wos: 1.96 and 1.99 dpm/100L). Overall, these results indicate strong reproducibility for the radium collection and counting process, and we found that radium-224 can be measured efficiently and accurately using the methods described here. The same cannot be said for radium-223.

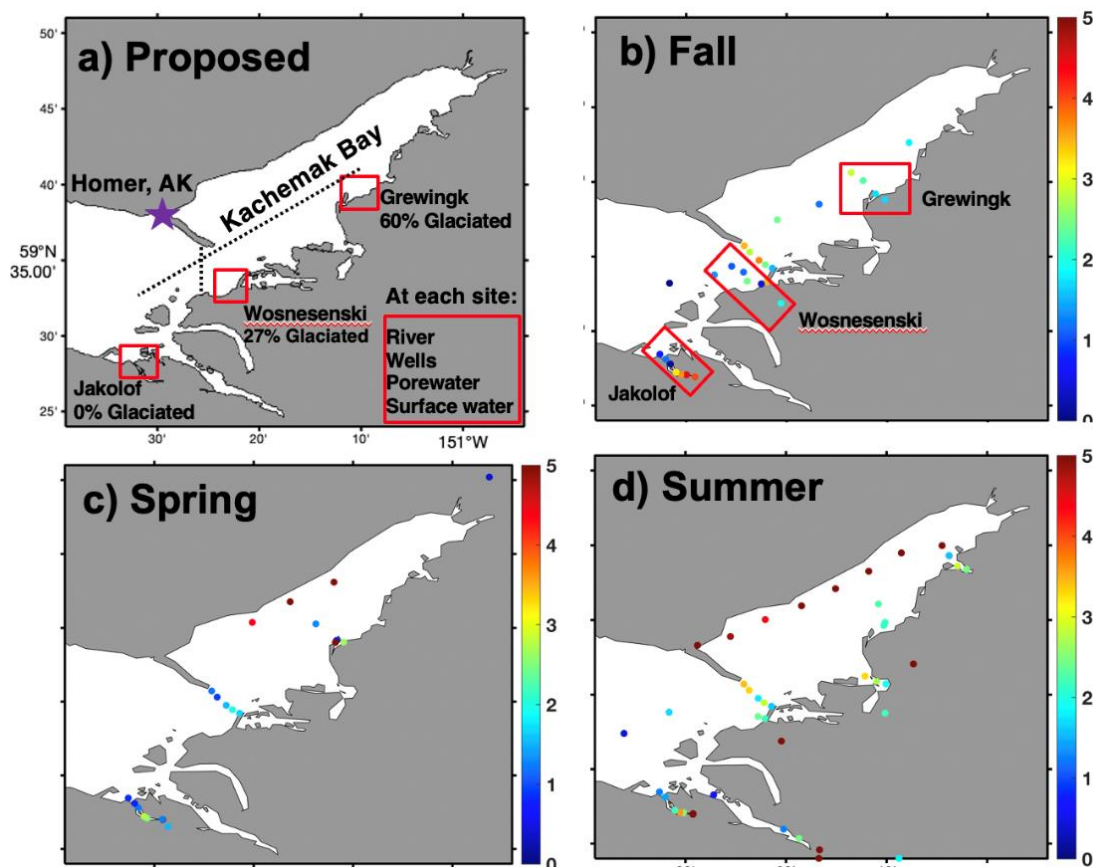


Figure 7: Radium surveys as planned (a) and carried out in the fall (b), spring (c), and summer (d). Colored dots are radium-224 activities in units of disintegrations per minute (dpm) per 100L. The percentages of glaciation in the watersheds were provided by Jenckes (pers. comm.).

Radium-223 activities are often $\sim 10\times$ lower relative to radium-224 (Moore, 2008), which was consistent in our study, with activities during fall 2020 ranging from 0.004–0.09 dpm/100L. Radium activities this low result in a low number of counts registered by the RaDeCC, and in turn, very large relative uncertainties. This became apparent during our initial fall 2020 survey, where relative uncertainties ranged from 48–592 %. Given these high uncertainties, little confidence could be applied to any radium-223 data interpretations and these data were deemed unusable. As a result, the values are not reported or interpreted here. The only remedy for this would be to

drastically increase sample volumes (~500 L), which would create unreasonable logistics. This has important implications for the residence time calculations (Objective 2), which are discussed below.

Constructing Radium and Nutrient Budgets via Mass Balance (Objective 1)

Objective 1 of the proposed work focused on building radium mass balances in Kachemak Bay. Closely following the survey originally proposed, radium and nutrient samples were collected in Jakolof Bay and the river plumes of Wosnesenski and Grewingk rivers, as well as across the Homer Spit transect and the longer along-bay transect.

Mass balances across Jakolof, Grewingk, and Wosnesenski sub-bays

The results of the fall survey (Figure 7b) showed few discernable patterns in radium-224 activities in the Wosnesenski and Grewingk river plumes. For example, at Grewingk, activities ranged very little (1.18–2.85 dpm/100L) with higher values found further from the shore (i.e., opposite from anticipated). These somewhat inconclusive results are likely due to the bathymetry of these two outflows; the rivers both exit into the open Kachemak Bay so no real sub-bays exist. This open geometry also leads to relatively coarse-grained underlying sediment (sand/pebbles) in these areas, making sediment grabs impossible to obtain. Given these early results, it became clear that creating mass balances in these very open systems was not feasible.

A mass balance could be constructed for Jakolof Bay. Radium-224 activities in the more classically-shaped Jakolof Bay (a longer more protected embayment) showed a clear pattern that matched a typical radium distribution. That is, a decreasing trend with distance away from the head of the bay (Figure 7), which was also present in Tutka Bay, though further investigation would be needed to create the radium mass balance (i.e., groundwater endmember samples, and water residence time estimates). The pattern in Jakolof Bay indicates a radium source at the head of the bay, presumably from groundwater and/or the Jakolof River. Given that the Jakolof River is relatively small, it was more likely this signal is driven by groundwater inputs.

Cross-bay sampling to constrain F_{mix}

The transect separating inner and outer Kachemak Bay conducted in all three seasons showed somewhat variable results. In the initial fall survey, results were as expected, with cold salty water (assumed to originate offshore) at the southern edge containing lower Ra-224, and water at the northern edge being warmer and fresher (presumably due to transit through the inner bay) and containing higher radium-224 (Figure 8). It appears an enrichment of approximately 2 dpm/100L occurs while waters transited through the bay, which is reasonable given the activities we observe throughout the bay (Figure 7). However, results from the spring and summer surveys were less conclusive (Figure 9). In spring, radium-224 showed little variability (ranging from 0.9–2 dpm/100L) and had a pattern opposite to that of the fall, which is unsurprising given the effects of the spring freshet. Increased surface water flow in spring and early summer would likely dominate over the groundwater flux and perhaps mask the baseline circulation in the bay that would be more pronounced in other seasons. In summer, the pattern was closer to that seen in the fall, but high-

activity waters near Homer Spit were not discernably warmer or fresher than waters nearer the southern coast, making it difficult to link the activities to flow (i.e., higher activities to outflow, lower activities to inflow). Overall, sampling across the Homer Spit transect did not yield clear enough patterns to elucidate radium activities in the inflowing and outflowing waters of Kachemak Bay, and thus could not be used to constrain F_{mix} .

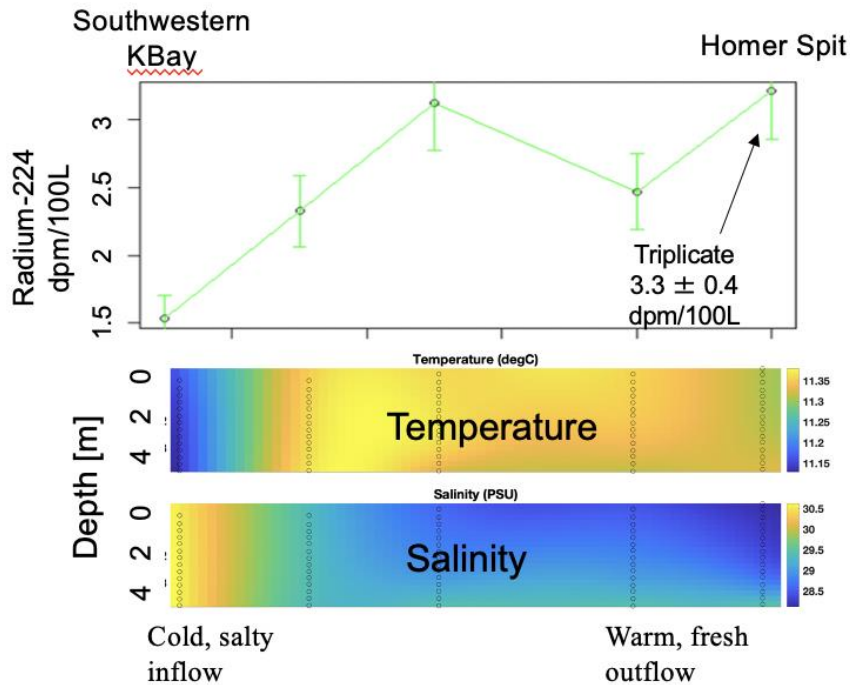


Figure 8: Radium activities (top) and temperature and salinity (bottom; upper 5m across the transect) across the Homer spit transect during fall 2020.

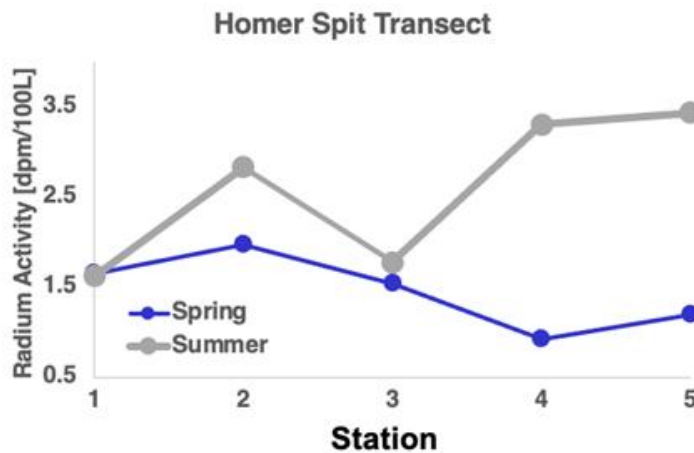


Figure 9: Spring and summer radium data across the Homer spit transect.

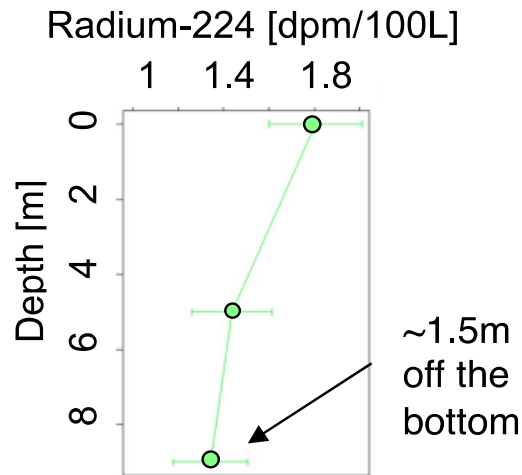


Figure 10: Vertical radium profile from Jakolof Bay station J4. No discernable sediment radium source is indicated.

The original proposal surmised that the sediments and rivers would present the most important terms in the radium mass balance. Indeed, the generally low radium signal leads to ingrowth term (F_{ingrowth}) and decay terms (F_{decay}) being relatively small, and estimating these values is relatively straightforward (although it's important to note that both terms would include a sizeable error due to the variability in radium activities measured across the bay). The results described in more detail below reveal that the F_{sediment} term is relatively small, but the F_{rivers} term is both large and difficult to constrain.

The flux from sediments ($F_{\text{sediments}}$) was deemed a relatively unimportant term. This was assessed in two ways. First, a vertical radium profile was taken in Jakolof Bay (at J4). The profile, shown in Figure 10, shows lower activities in the subsurface waters, and no discernable increase near the bottom. This would imply a relatively unimportant seafloor radium source.

Second, bottom sediments collected from the same location and incubated in the laboratory (see Methods) revealed a relatively low diffusive flux of radium from sediment. Details of these incubation results are described in detail in the Jakolof mass balance section below. In short, the flux of radium out of bottom sediments was shown to be an insignificant term in the radium mass balance. It is important to note, however, that these samples were taken in Jakolof Bay and cannot be entirely representative of seafloor sediments across Kachemak Bay. That said, much of Kachemak Bay is relatively deep (averaging 46 m, maximum depth 176 m) and, in these areas, radium-224 diffusing from the seafloor will mostly decay before impacting surface water activities.

Constraining the flux from rivers (F_{rivers}) was much more difficult than anticipated. The results showed the riverine flux to be very large and highly variable both spatially and temporally. Riverine samples were taken from six rivers across Kachemak bay, with some sampled in three seasons. Riverine radium activities were first collected from three rivers during the fall survey. These activities were generally low (Table 2), except in the Jakolof River. Differences across the

three rivers indicated radium activity may vary with percent watershed. The fall survey generated two differing hypotheses. The first hypothesis was promising in regards to Objective 1: the riverine radium activity is generally low, meaning higher activities seen in surface waters across the bay are driven by a groundwater signal. From this, we inferred that the SGD from the extensive mudflats at the head of Kachemak Bay (near Fox River) could be a dominant radium source in the bay. The second hypothesis was that much of the radium in rivers is adsorbed to fine-grained particulates, which prevents extraction onto the MnO₂ fiber, resulting in an underestimation of riverine radium during the fall survey. In this case, underestimation should be greatest at Grewingk, a glacially-fed river with high loads of suspended particulates (i.e., glacial flour). We observed very low radium-224 at this location in the fall.

Table 2: Riverine radium-224 activities measured across Kachemak Bay. Dissolved radium is measured by extracting radium directly from the freshwater (S=0), whereas total riverine radium is measured by salting the river water before radium extraction.

| River | % Watershed Glaciation | Dissolved Radium (Salinity = 0) | Dissolved Radium (Salinity = 0) | Dissolved Radium (Salinity = 0) | Total Radium (Salinity = 20) | Total Radium (Salinity = 20) |
|----------|---------------------------|------------------------------------|------------------------------------|------------------------------------|---------------------------------|---------------------------------|
| | | Ra-224 Fall | Ra-224 Spring | Ra-224 Summer | Ra-224 Spring | Ra-224 Summer |
| Jakolof | 0 | 4.01 | 0.22 | 0.37 | 3.95 | 5.57 |
| Grewingk | 60 | 1.68 | 0.70 | 1.47 | 4.11 | 7.29 |
| Wos | 27 | 1.98 | - | 1.73 | - | 7.09 |
| Foxe | 16 | - | 0.38 | | 8.81 | - |
| Halibut | 8 | - | - | 1.83 | - | 7.91 |
| Tutka | 16 | - | - | 0.42 | - | 5.39 |

Strong sediment adsorption of radium in freshwater has been documented previously (Moore et al., 2008). Briefly, in waters with low ionic strength (i.e., fewer ions, as in freshwater), radium is strongly sorbed to sediments, but when ionic strength increases (i.e., salinity increases), those ions will sorb more strongly to particle surfaces, releasing dissolved radium into the saline water column. With this in mind, measuring the total riverine radium activity onto the MnO₂ fiber requires that a saline environment be induced by ‘salting’ the river sample prior to radium extraction.

The river salting experiment yielded a zero-salinity sample (duplicating our method from the previous fall) with low radium activity (0.7 dpm/100L), lower than the fall sample (1.68 dpm/100L). As shown in Figure 11, we found a clear linear increase in riverine radium activity, up to a threshold of salinity of ~15 where activities were ~6x higher (4.3 dpm/100L) compared to the unsalted sample. This provides two clear results: (1) salting of a river sample is imperative to measure the ‘true’ riverine radium endmember and, more importantly here, (2) rivers were a considerably larger radium source than initially considered following the fall survey. All subsequent river samples were collected in duplicate to provide a fresh sample to assess the

‘dissolved’ riverine radium fraction and one sample to be salted to 20 to assess the total radium activity. These samples revealed high total activities in all rivers as well as considerable variability between rivers (ranging from 3.95–8.81 dpm/100L, see Table 2). In summary, our results show that Kachemak Bay rivers contain large radium activities, that activities vary considerably between rivers and between seasons, and that some larger rivers, which are not monitored for discharge due to lack of accessibility, exhibit seemingly high activities (e.g., Fox River at the head of the bay).

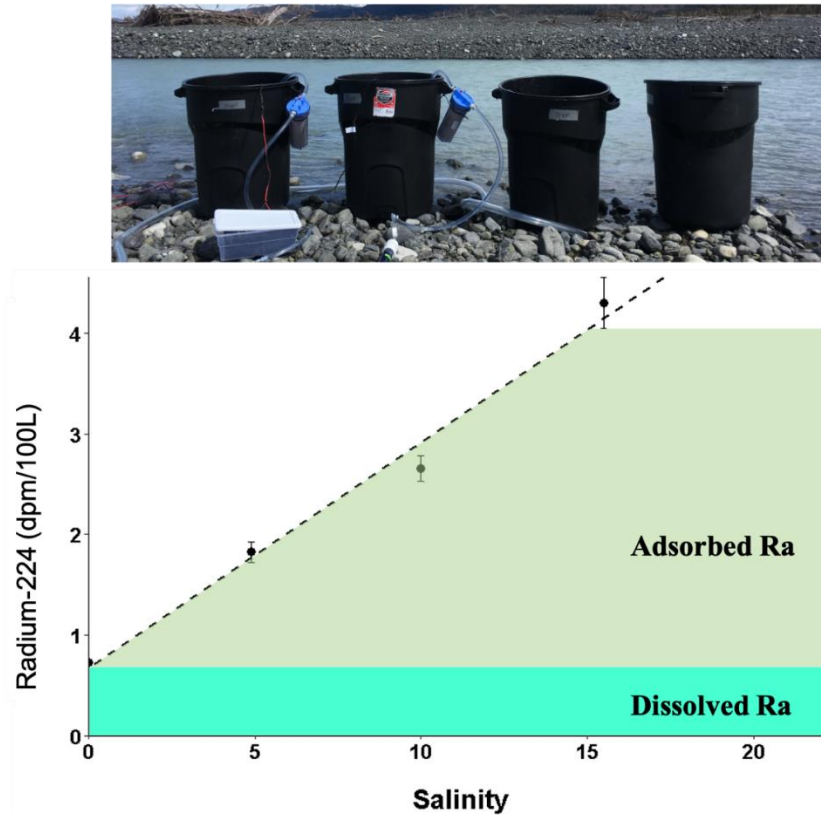


Figure 11: Photo of salting experiment samples on the Grewingk River bank (top) and graph showing experiment results (bottom). Results show a linear increase in radium activity with increasing salinity up to a threshold at 15, where ionic strength is high enough for all radium to desorb from particulates.

Groundwater radium endmembers

A total of seven groundwater samples were collected from temporary PVC wells during the spring and summer surveys, six from Jakolof Bay and one from the north side of Kachemak Bay. In spring, five temporary wells were deployed in the upper mudflats of Jakolof Bay. Wells were placed in a T-shaped array, providing a 3-point transect both across the mudflat and up/down the slope. In summer, a single well was deployed in a similar part of the mudflats. Groundwater activities in these six wells varied considerably and were strongly correlated with salinity ($R^2 = 0.93$, linear fit is forced through the origin, Figure 12). This strong relationship is likely driven by radium’s affinity to particles at low salinity (as seen in the river data). Utilizing our results from the

river salting experiment, we can estimate the total radium activity that this fresh groundwater will introduce upon entering the marine system by extrapolating this relationship up to the salinity 15 threshold, yielding a Jakolof Bay groundwater endmember of 25.95 dpm/100L.

During the summer survey, a single PVC well was installed in the mudflats that extend along the north side of Kachemak Bay. There, we observed a groundwater radium-224 of 67.27 dpm/100L. Salinity in this well read 14.5, thus assuming the vast majority of radium has desorbed from particles, this result implies that groundwater entering along the north coast of Kachemak Bay is ~2.6x more enriched in radium-224 compared to the Jakolof Bay mudflats. This enrichment along the north coast aligns well with our observation of high radium-224 in surface waters along the north coast of Kachemak Bay during spring and summer (Figure 7). Indeed, our summer transect along the entire north coast of the bay yielded consistently high radium-224 (4.4-6.6 dpm/100L) with no discernable correlation with salinity (i.e., not primarily a riverine signal). Based on these findings, it appears that SGD from mudflats along the northern coast may be an important (and possibly the largest) source of radium in this system.

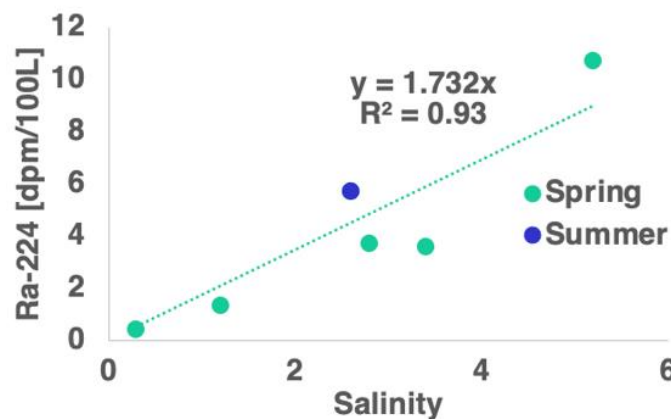


Figure 12: Relationship between groundwater radium and salinity in the Jakolof Bay wells.

Nutrient data across Kachemak Bay

In total, 96 nutrient samples were collected in the surface seawater across Kachemak Bay for nitrate, ammonium, phosphate, and silicic acid. Results were highly variable, with few consistent patterns. The highest values were found in river and groundwater samples, with the highest value recorded from the Fox River. This is notable because Fox River is not sampled by any ongoing field program in Kachemak Bay, yet it may be a key nutrient source to the bay. However, it should be noted that these nutrient samples (triplicate samples) were transported for many hours on ice before being frozen, which could have impacted the results. Generally, lower nutrient concentrations were observed in summer compared to spring and fall, likely due to increased stratification of the water column in July. Key nutrient endmembers for groundwater and river water, as well as nutrient samples along the offshore transect, are described in more detail below.

Radium mass balance in Jakolof Bay

Many of the results described above, in particular the convoluted nature of the riverine flux, led us to the conclusion that constructing a reliable radium mass balance for the whole of Kachemak Bay within the required timeframe of this project would not be feasible. Instead, we focused our study in Jakolof Bay, where favorable bay geometry, promising preliminary radium data, and the presence of the relatively small Jakolof River provided the best opportunity to test the radium-based approaches outlined in the original proposal.

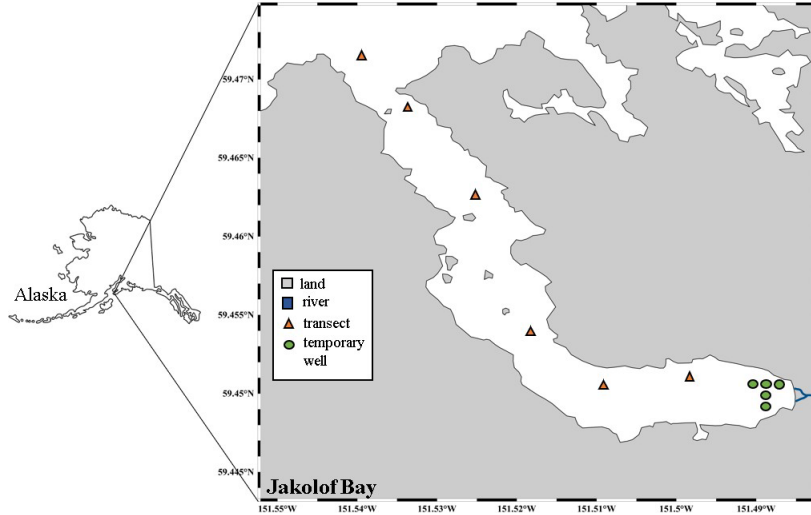


Figure 13: Jakolof Bay sampling stations. Locations for the 6-station sampling transect are shown (orange triangles). The green circles indicate the temporary PVC wells deployed in the mudflat and the Jakolof River (thick blue line) is shown at the head of the bay.

Table 3: Radium mass balance terms, and resulting SGD calculation.

| Survey | F_{mix} (dpm/day) | F_{decay} (dpm/day) | F_{river} (dpm/day) | F_{sed} (dpm/day) | F_{gw} (dpm/day) | $[^{224}\text{Ra}]_{\text{GW}}$ (dpm/100L) | SGD (m ³ /day) | SGD (cm/day) |
|--------------------|-------------------------------|---------------------------------|---------------------------------|-------------------------------|------------------------------|---|------------------------------|-----------------|
| Fall | 4.40E+07 | 3.30E+07 | 1.1E+07 [#] | 4.30E+05 | 6.60E+07 | 25.95 [*] | 2.60E+05 | 36.1 |
| Spring (Low_Tide) | 1.20E+07 | 1.40E+07 | 2.20E+06 | 3.50E+05 | 2.30E+07 | 25.95 | 9.00E+04 | 12.8 |
| Spring (High_Tide) | 1.30E+07 | 2.10E+07 | 2.20E+06 | 5.00E+05 | 3.10E+07 | 25.95 | 1.20E+05 | 16.8 |
| Summer | 2.60E+07 | 2.20E+07 | 1.30E+06 | 3.60E+05 | 4.60E+07 | 25.95 | 1.80E+05 | 25 |

[#] riverine radium endmember estimated using spring and summer data

^{*} estimated based on spring and summer data (see Figure 12)

The Jakolof Bay radium sources (F_{river} , F_{sed} , F_{gw}) and sinks (F_{mix} , F_{decay}) (i.e., the mass balance) were constructed for all four surveys (Figure 13), with results summarized in Table 3. For the fall survey, averages of spring/summer data are used to fill in critical gaps (e.g., groundwater radium endmember), so results for this season have a larger uncertainty. In spring, radium surveys were completed at high and low tides to assess variability over a tidal cycle. Riverine fluxes were highest in fall and lowest in summer, predominantly driven by changes in discharge rates. The per-square meter flux from bottom sediments was assumed to be

constant across all seasons, but this value was then multiplied by the area of the submerged seafloor, which differs depending on the tidal stage, thus F_{sediment} varied slightly across the four surveys. Overall, F_{sediment} is 1–2 orders of magnitude lower than other mass balance terms and thus is deemed a negligible source to Jakolof Bay. For the F_{mix} , $F_{\text{supported}}$, and F_{decay} terms, the average activity inside the bay was taken as the average value across the first five stations along the Jakolof bay, with the outermost station along the Jakolof Bay transect (J6, located outside the Bay, see Figure 13) representing the ‘outside the bay’ activity.

Combining all terms in the mass balance (following Eq. 1 above) yielded F_{gw} values ranging from $2.3\text{--}6.6 \times 10^7$ dpm/day. Incorporating the radium groundwater endmember (see above) and following Eq. 2 (above) yielded groundwater discharges of $0.9\text{--}2.6 \times 10^5$ m³/day. These values represent the total volume of groundwater discharged into Jakolof Bay per unit of time. By dividing by the area of the mudflat where we presume this groundwater emanates from (i.e., the seepage face), which was calculated by Aeon Russo (pers. comm), a cm/day unit of groundwater flux can also be calculated. The seepage face was determined by tracing the coastline at mean tide level for the head of the bay and calculating the area of the intertidal. This area was divided by the coastline length to get an average drainage length which was used to calculate the seepage face when the slope of the intertidal was considered to be 50 degrees from the bathymetry. The coastline length was then multiplied by the length of the seepage face.

The highest SGD was calculated in fall, however, multiple terms in the fall mass balance were assumed based on the spring and summer data. Focusing instead on the 2021 surveys, total SGD increased by ~50% from spring to summer, driven by a change in the F_{mix} term. Spring SGD was measured at both high and low tides, while summer SGD is based on data collected at a tidal stage that lies between the low and high tides. Spring data does not reveal any meaningful difference between SGD at different tidal stages (0.9×10^4 m³/day at low tide, and 1.2×10^4 m³/day at high tide), suggesting that a different tidal stage is not responsible for the differing SGD results. Lecher et al. (2016) assumed that SGD is the same throughout the year due to tides driving SGD, but this might not be the case in Jakolof Bay. The river flux in Jakolof Bay is highest in late May with a maximum of 2.49 m³/s which then decreases to zero in August (Jenckes et al., in prep).

The SGD estimates calculated here are considerably lower than those calculated estimates calculated previously in nearby Kasitsna Bay (average = 130–260 cm/day, Lecher et al., 2016; Dimova et al., 2015). This is somewhat unsurprising given that Kasitsna Bay beach is underlain by more permeable rocky sediment compared to the Jakolof Bay mudflats. In contrast to Kasitsna Bay, our reported SGD rates (13–36 cm/day, Table 3) are comparable but slightly higher than the median SGD rates reported throughout the Pacific (2–22 cm/day) and Atlantic Oceans (1–10 cm/day) (Santos et al., 2021). These comparisons show that, as hypothesized, SGD is relatively large in this region, likely due to the presence of large tides. These comparable results provide confidence in the radium-based mass balance approach taken here.

Nutrient fluxes in Jakolof Bay

Nutrient data was also measured from rivers, seawater, and groundwater in Jakolof Bay during all three surveys. These data are summarized in Table 4. The highest nitrate concentrations were consistently found in the river, while for phosphate highest concentrations were found in seawater (i.e., both rivers and groundwater are relatively phosphate depleted). Consequently, the nitrate-to-phosphate ratios (N:P) are very high in riverine and groundwater, and relatively low in seawater. This ratio helps predict the availability of the nutrient source to be taken up by photosynthesizing organisms (i.e., phytoplankton) because phytoplankton typically take up these nutrients in specific ratios. The N:P in seawater was roughly 2x higher in spring compared to summer and fall, and considerably closer to the organismal ratio of 16, suggesting more favorable growing conditions existed during spring (May). However, the N:P in Jakolof Bay is < 10 throughout the year (Table 4), implying that nitrate is the major limiting nutrient. Similar seasonal trends in N:P ratios are found in nearby Seldovia Bay (data at <https://cdmo.baruch.sc.edu>). In summer, seawater has a very low N:P (~ 3), implying that phytoplankton growth is limited by the availability of nitrogen, which is considered the primary limiting nutrient throughout much of the global ocean.

Table 4: The concentration of nutrients in the river and groundwater across seasons in Jakolof Bay. Groundwater samples were taken from a temporary PVC well at ebb tide. The associated uncertainty is the standard deviation of the replicates.

| Source | Season | NO ⁻ (μM) | NH ⁺ (μM) | PO ³⁻ (μM) | SiO ²⁻ (μM) | N:P |
|--------------|-----------|----------------------|----------------------|-----------------------|------------------------|--------|
| River water* | Sept 2020 | 9.95 | 0.42 | 0.07 | NA* | 145.23 |
| Seawater** | Sept 2020 | 3.50 ± 0.76 | 0.76 ± 0.08 | 0.74 ± 0.09 | 10.00 ± 2.56 | 4.73 |
| River water | May 2021 | 22.35 ± 0.27 | 0.24 ± 0.03 | 0.04 ± 0.01 | 108.02 ± 0.88 | 615.23 |
| Groundwater | May 2021 | 5.50 ± 3.02 | 0.87 ± 0.28 | 0.09 ± 0.03 | 64.74 ± 20.4 | 63.43 |
| Seawater*** | May 2021 | 5.39 ± 1.56 | 1.08 ± 0.21 | 0.66 ± 0.16 | 14.39 ± 3.96 | 8.17 |
| River water | July 2021 | 9.81 ± 0.07 | 0.39 ± 0.26 | 0.05 ± 0.01 | 98.2 ± 1.52 | 196.20 |
| Groundwater | July 2021 | 7.50 ± 0.68 | 0.75 ± 0.08 | 0.22 ± 0.02 | 119.88 ± 2.44 | 34.09 |
| Seawater** | July 2021 | 1.43 ± 1.17 | 1.26 ± 0.28 | 0.43 ± 0.13 | 23.94 ± 30.08 | 3.33 |

* No replicates done in fall 2020

** One replicate done at each of the 6 stations along the transect in Jakolof (n=6)

*** Transect done at low and high tide (n=12)

When considering the ratio of nitrate and nitrite to phosphate (N+N:P), the same trends are seen as the N:P above. Furthermore, the N:P values are between 91% and 99% of the N=N:P values which demonstrates that we can use N:P as a proxy for the total nitrogen to total phosphorous ratio. Combining these nutrient endmembers with the groundwater discharges calculated above yielded groundwater nutrient fluxes for all surveys. These values, as well as comparable values for river fluxes, are summarized in Table 5.

Table 5: Nitrate, phosphate, and silicic acid fluxes from the Jakolof river (riverine) and the Jakolof mudflats (groundwater) across fall, spring, and summer seasons.

| Compound | Season | Porewater Concentration (mol/m ³) | Groundwater Flux (mol/day) | Riverine Concentration (mol/m ³) | Riverine Flux (mol/day) |
|--------------|--------------------|---|----------------------------|--|-------------------------|
| Nitrate | Fall | 0.0065* | 1660 | 9.95E-03 | 2755 |
| Nitrate | Spring (Low Tide) | 0.0055 | 496 | 2.24E-02 | 1236 |
| Nitrate | Spring (High Tide) | 0.0055 | 655 | 2.24E-02 | 1236 |
| Nitrate | Summer | 0.0075 | 1326 | 9.81E-03 | 229 |
| Phosphate | Fall | 0.00016* | 39.6 | 0.00007 | 19.4 |
| Phosphate | Spring (Low Tide) | 0.00009 | 8.1 | 4.00E-05 | 2.2 |
| Phosphate | Spring (High Tide) | 0.00009 | 10.7 | 4.00E-05 | 2.2 |
| Phosphate | Summer | 0.00022 | 38.9 | 0.00005 | 1.2 |
| Silicic Acid | Fall | 0.09231* | 23568 | 0.103 | 28522 |
| Silicic Acid | Spring (Low Tide) | 0.06474 | 5844 | 1.08E-01 | 5973 |
| Silicic Acid | Spring (High Tide) | 0.06474 | 7705 | 1.08E-01 | 5973 |
| Silicic Acid | Summer | 0.11988 | 21194 | 0.0982 | 2291 |

*average of the spring and summer data

For nitrate, river fluxes were 2–3x higher than groundwater in fall and spring, when river discharges are higher. In summer, when river discharges are low, groundwater nitrate-flux outweighs the river flux by a factor of 6. As mentioned above, summertime phytoplankton growth in Jakolof Bay appears to be nitrate-limited, suggesting that this groundwater nitrate source is critical to help sustain biological activity during much of the area’s relatively short growing season. In other words, groundwater fluxes help to buffer against seasonal variations in seawater nitrate.

Silicic acid concentrations ($[\text{SiO}_4^{2-}]$) in porewaters during spring and summer ($64.74 \pm 20.4 \mu\text{M}$ and $119.88 \pm 2.44 \mu\text{M}$, respectively) were statistically significantly higher than silicic acid concentrations in seawater (see Table 4, Tukey-Kramer test $p < 0.05$), pointing to SGD as an important source of silicic acid to the water column. Indeed, consistent declines in seawater $[\text{SiO}_4^{2-}]$ with distance offshore (not shown) imply a source at the bay’s head, and calculated SGD silicic acid fluxes were comparable to (fall and spring) or much higher than (~10x in summer) river fluxes.

Phosphate fluxes from groundwater appear to be larger than riverine fluxes across all four sampling surveys, indicating that groundwater is a more important source of phosphate to Jakolof Bay compared to rivers. However, these fluxes are very small relative to nitrate

and silicic acid fluxes, and the magnitude and spatial pattern of seawater phosphate concentrations ($[\text{PO}_4^{3-}]$) indicate that neither groundwater nor rivers play an important role in the phosphate budget. The tidal-pumping mechanism will release groundwater to the marine system during ebb tide, thus the groundwater signal should be highest at low tide. However, in spring, seawater $[\text{PO}_4^{3-}]$ in Jakolof Bay was significantly lower at low tide (0.34–0.64 μM) compared to high tide (0.58–0.87 μM), and was considerably higher than groundwater $[\text{PO}_4^{3-}]$ ($0.09 \pm 0.03 \mu\text{M}$). Similar results were found in summer, with seawater $[\text{PO}_4^{3-}]$ at flood tide ranging from 0.18–0.55 μM ($0.43 \pm 0.13 \mu\text{M}$, $n=6$) and groundwater $[\text{PO}_4^{3-}]$ of $0.22 \pm 0.02 \mu\text{M}$. These results suggest that tidally-driven SGD acts as a net phosphate sink in Jakolof Bay and tidal pumping of seawater into and out of the mudflat region may remove phosphate from seawater. This could occur if iron and manganese oxides form and bind to phosphate that enters the aquifer on the flood tide (Lecher et al., 2016). With SGD deemed a phosphatesink, and river fluxes extremely low, the dominant source of phosphate to Jakolof Bay is almost certainly offshore waters originating from the Alaska Coastal Current (ACC). This is supported by the observation of higher seawater $[\text{PO}_4^{3-}]$ at high tide (0.74 μM , when the signal of offshore waters is greater) relative to low tide (0.52 μM). The ACC is typically nutrient-rich due to interactions with deeper waters as it passes over the continental shelf before entering Kachemak Bay (Stabeno et al., 2004).

Calculating offshore fluxes

In fall 2020, samples were collected along a 30km transect extending from the middle of inner Kachemak Bay to the outer bay. These data are shown in Figure 14. Radium activities varied within the bay, with the peak activity observed at Homer spit (Figure 14b). Further offshore, radium decreased sharply to a minimum of 0.28 dpm/100L. Using a subset of the transect that extends offshore from Homer Spit (Figure 14c), a slope of -0.2694 corresponds to a horizontal diffusivity (K_x) of 30 m^2/s . This diffusivity is at the lower end of values calculated using similar methods in other regions (e.g., Moore, 2008; Burt et al., 2013b). Despite obtaining this calculated diffusivity, nutrient concentrations showed no discernable gradients across these four stations, thus calculation of offshore fluxes using Ficks Law (see Methods) was not possible. Overall, these results are promising in terms of the future feasibility of this approach.

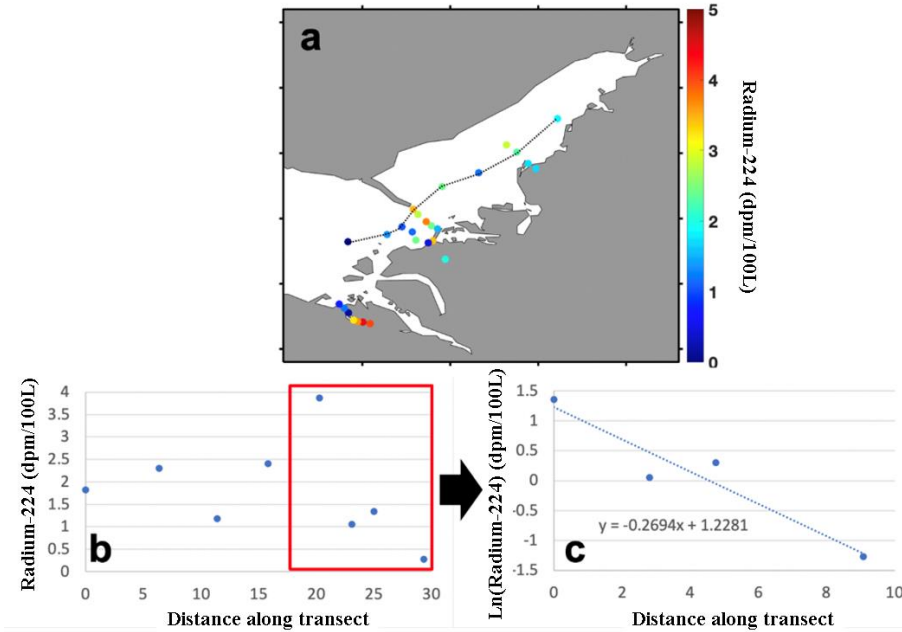


Figure 14: Radium-224 measured along Kachemak Bay transect during fall 2020: (a) Radium-224 (in dpm/100L) along the offshore transect in the fall survey, (b) the activity plotted with distance along the transect (The outer part of the transect where radium declines steeply is outlined by the red box), and (c) the natural log of the radium activity plotted with distance along the outer part of the transect. Slope of the linear fit is used to calculate horizontal mixing rates.

Residence Time (Objective 2)

The inability to accurately measure Ra-223 leads to an inability to use Ra-223 in the isotope ratio technique for residence time estimation. This was a major setback in regard to Objective 2, as it required us to consider one of the longer-lived radium isotopes (radium-226 and radium-228) rather than radium-223. Although long-lived radium isotopes are also effectively extracted from seawater using MnO₂ fibers, and thus present on our samples, they cannot be measured using the RaDeCC, and the instrumentation required is not available at UAF. We collaborated with the University of Hawaii-Manoa (Dr. Henrietta Dulai) to analyze our MnO₂ fibers for long-lived radium. We obtained radium-228 and radium-226 data for a subset of samples along the Jakolof Bay transect, as well as for the Jakolof groundwater endmember. The ratio of radium-224, to either radium-226 or 228, is a commonly used method for nearshore residence time because the activity of radium is typically 1–3 orders of magnitude greater in groundwater than in seawater (Garcia-Orellana et al., 2021, and many others). In Jakolof Bay, the radium-224 groundwater endmember was ~10x greater than seawater; however, the radium-226 in groundwater was found to be 3–4x lower than seawater (2.02 ± 0.96 dpm/100L in groundwater versus 8.20 ± 2.12 dpm/100L in seawater) and the radium-228 in groundwater was slightly lower than seawater (0.81 ± 1.41 dpm/100L in groundwater versus 2.38 ± 1.23 dpm/100L for seawater). Additionally, during the spring and summer surveys, radium-226 increased linearly with distance away from the head of the bay (Figure 15b), indicating that offshore waters are a source of radium-226 to Kachemak Bay. Radium-228 showed mixed results, with two of four

surveys yielding higher radium-228 offshore (Figure 15c). Unsurprisingly, residence time calculations via Eq. 5 yielded decreasing water-mass ages with distance away from the mudflats, which is counterintuitive to the assumption that the primary radium source is the mudflats. These results indicate that two of the three key assumptions required for radium-based residence time calculations have been violated: that the radium isotopes measured enter the bay from a single dominant source and that the offshore water is depleted in radium. With this in mind, our results show that radium-based residence time is not a feasible approach in the Cook Inlet region. However, the tidal prism approach yielded a Jakolof Bay residence time of 0.6–0.7 days (15–17 hours) across all three seasons.

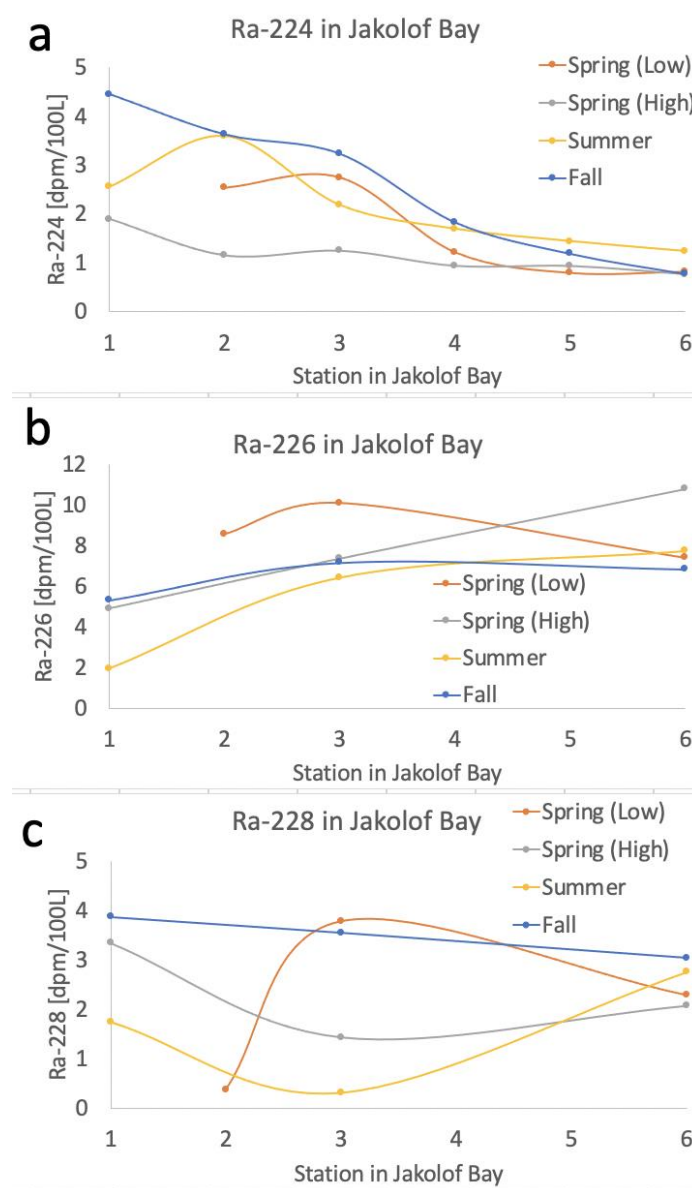


Figure 15: Activities of radium-224 (a), radium-226 (b), and radium-228 (c) along the Jakolof Bay sampling transect for all three seasons. Spring samples were also taken at high and low tides.

DISCUSSION

Discussion on the detailed results is provided in the previous sections. Here, we address the overarching outcomes about the feasibility of radium-based approaches in the Cook Inlet region.

Objectives 1 and 2

Outcomes for the radium and nutrient budgets across Kachemak Bay were mixed. Overall, radium activities in this region were on the lower end of values when compared to other coastal and nearshore studies. For example, radium activities from a similar bay setting along the great barrier reef were approximately 10x higher (Hancock et al., 2006). This created significant logistical challenges: the need to collect very large volumes for detection, extensive time needed to adequately count samples on the RaDeCC (leading to sample backlogs), and the inability to measure radium-223 (discussed below). Despite these challenges, this report outlines robust and detailed methodologies for radium collection and analysis that can be utilized going forward.

Radium budgets could not be created in most areas around Kachemak Bay because basin geometry prevented isolation of land-based sources. Additionally, accurate radium budgets could not be obtained for most of Kachemak Bay due to the complicated nature of the riverine inputs and inconsistent results measured across the Homer Spit transect that made it difficult to constrain the F_{mix} term. Instead, focused our study on Jakolof Bay. Here, results were excellent, with all mass balance terms well-constrained and intriguing results regarding the magnitude of groundwater discharge and the relative importance of seafloor, river, groundwater, and offshore sources for critical nutrients. These results show that radium-based approaches can produce useful results when applied in the right system. Based on this proof-of-concept study, the creation of a meaningful mass balance in outer Kachemak Bay may only be attainable by understanding the magnitude and variability of the riverine radium signal in this area and conducting an extensive sampling effort to properly constrain all the important river and groundwater endmembers.

The results from our study indicate that the general approach of using radium to calculate offshore fluxes is feasible in this region. If conducting work near Kachemak Bay, transects should begin at Homer Spit and extend further offshore. In Cook Inlet, transects could begin near the mouth of the Inlet. Regardless of the specific area, larger sample volumes (>500L) will be required due to the very low activities observed in these offshore waters.

Regarding Objective 2, the fall 2020 survey provided clear evidence that the proposed residence time approach (using radium-224:radium-223 ratios) would not be feasible due to analytical/logistical issues surrounding radium-223. Pivoting to using a longer-lived radium approach required significant laboratory work to prepare samples for analysis and travel to the University of Hawaii to get samples analyzed. Results of that work showed that offshore waters are enriched in long-lived isotopes, thereby violating a key assumption needed for residence time calculations. These data, while not yielding a result for Objective 2, provide critical baseline measurements of the radium quartet (radium-224, 223, 226, and 228) that will shape future studies in this region. Finally, in light of these results, we successfully estimated residence time in Jakolof Bay using the more traditional tidal prism approach. Similar approaches could be taken for other areas of Kachemak Bay, or perhaps for the entire bay itself.

Local Involvement and Scientific Outreach

Two of the three proposed efforts for outreach and local involvement were achieved, albeit with limited scope due to the ongoing pandemic. First, we conducted virtual classroom visits and public lectures, including multiple presentations/discussions with three schools in the Chugach School District (November/December 2020) and a public presentation at the Kachemak Bay Science Conference (March 2021). Second, engagement with members of the Seldovia Village Tribe informed our team whether our field activities were viewed positively by the local community, provided local knowledge regarding our study site, and sparked discussions of how our science might benefit the local community in the future (e.g., use in predicting harmful algal blooms). In 2022, project results were presented virtually to members of the Seldovia Village Tribe, Kodiak Area Native Association, and the Alutiiq Pride Marine Institute.

ACKNOWLEDGMENTS

A major thank you to Ana Aguilar-Islas, Lee-Ann Munk, Natalie Monacci, UAF College of Fisheries and Ocean Sciences, and the Cook Inlet Regional Citizens Advisory Council who all committed cost share for this project. This work could not have been done without support from the EPSCoR Fire & Ice Project members Katrin Iken, Brenda Konar, LeeAnn Munk, and many others, and from the Kasitsna Bay Laboratory staff, who helped tremendously in collecting our data. Many thanks to graduate student Josianne Haag, who took on many of the research activities for this project efficiently and professionally. This project was funded by the Alaska Coastal Marine Institute and the Bureau of Ocean Energy Management (M20AC10016).

STUDY PRODUCTS

- Burt, W. Why radium/radon is useful in KBay, Take 1. Kachemak Bay/Cook Inlet Marine Ecosystem Workgroup. Zoom presentation. October 2020.
- Burt, W. Characterizing groundwater input across a glacial gradient in Kachemak Bay using naturally-occurring radium isotopes. EPSCoR Fire and Ice All-Hands Meeting. Oral Presentation. November 2020.
- Burt, W. Radium/Radon in KBay: Results and future directions. EPSCoR Fire and Ice Coastal
Haag, J. Characterizing groundwater fluxes and water residence time using radioisotope tracers: Preliminary findings from Kachemak Bay, southeast Alaska. Poster presentation. Alaska Marine Science Symposium. January 2021.
- Burt, W. CMI Annual Review. Zoom presentation. January 2021.
- Burt, W. Digging into groundwater: Measuring marine radioactivity to unravel groundwater's role in ecosystem processes. Kachemak Bay Science Conference. Zoom presentation. March 2021.
- Haag, J. Characterizing groundwater in Kachemak Bay using naturally-occurring isotopes. EPSCoR Fire & Ice Coastal Margins meeting. Zoom presentation. September 2021.
- Haag, J. Investigating SGD as a key nutrient source in a high latitude macrotidal estuary using multiple approaches. Ocean Sciences Conference. Zoom presentation. February 2022.

REFERENCES

- Archer, A. 2013. World's highest tides: hypertidal coastal systems in North America, South America, and Europe. *Sedimentary Geology*, 284-285:1-25.
- Armstrong, F.A.J., Stearns, C.R., and Strickland, J.D.H. 1967. The measurement of upwelling and subsequent biological processes by means of the Technicon Autoanalyzer and associated equipment. *Deep-Sea Research*, 14:381-389.
- Brabets, T.P., Nelson, G.L., Dorava, J.M., and Milner, A.M. 1999. Water-quality Assessment of the Cook Inlet Basin, Alaska: Environmental Setting. Water-Resources Investigations Report 99-4025, US Department of the Interior, US Geological Survey. doi.org/10.3133/wri994025.
- Burbank, D.C. 1977. Circulation studies in Kachemak Bay and Lower Cook Inlet. In: Environmental studies of Kachemak Bay and Lower Cook Inlet, Volume III. Trasky, L.L., Flagg, L.B., and Burbank, D.C. (eds.). Alaska Department of Fish and Game Marine/Coastal Habitat Management, Anchorage, AK.
- Burnett, W.C., and Dulaiova, H. 2003. Estimating the dynamics of groundwater input into the coastal zone via continuous radon-222 measurements. *Journal of Environmental Radioactivity*, 69:21-35.
- Burt, W.J., Thomas, H., Fennel, K., and Horne, E. 2013a. Sediment-water column fluxes of carbon, oxygen and nutrients in Bedford Basin, Nova Scotia, inferred from ²²⁴Ra measurements. *Biogeosciences*, 10:53-66. doi.org/10.5194/bg-10-53-2013.
- Burt, W.J., Thomas, H., and Auclair, J.-P. 2013b. Short-lived radium isotopes on the Scotian Shelf: Unique distributions and tracers of cross-shelf CO₂ and nutrient transport. *Marine Chemistry*, 156:120-129. doi.org/10.1016/j.marchem.2013.05.007.
- Burt, W.J., Thomas, H., Hagens, M., Pätsch, J., Clargo, N. M., Salt, L. A., Winde, V., and Böttcher, M.E. 2016. Carbon sources in the North Sea evaluated by means of radium and stable carbon isotope tracers. *Limnology and Oceanography*, 61(2):666-683. doi.org/10.1002/lno.10243.
- Burt, W.J., Thomas, H., Pätsch, J., Omar, A.M., Schrum, C., Daewel, U., Brenner, H., and de Baar, H.J.W. 2014. Radium isotopes as a tracer of sediment-water column exchange in the North Sea. *Global Biogeochemical Cycles*, 28(8):786-804. doi.org/10.1002/2014GB004825.
- Dimova, N.T., Paytan, A., Kessler, J.D., Sparrow, K.J., Garcia-Tigres Kodovska, F., Lecher, A.L., Murray, J., and Tulaczyk, S.M. 2015. Current magnitude and mechanisms of groundwater discharge in the Arctic: case study from Alaska. *Environmental Science and Technology*, 49(20):12036-12043.
- Dulaiova, H., and Burnett, W.C. 2008. Evaluation of the flushing rates of Apalachicola bay, Florida via natural geochemical tracers. *Marine Chemistry*, 109(3-4):395-408.
- Garcia-Solsona, E., Garcia-Orellana, J., Masqu, P., and Dulaiova, H. 2008. Uncertainties associated with ²²³Ra and ²²⁴Ra measurements in water via a delayed coincidence counter (RaDeCC). *Marine Chemistry*, 109:198-219.

- Garcia-Orellana, J., Rodellas, V., Tamborski, J., Diego-Feliu, M., van Beek, P., Weinstein, Y., Charette, M., Alorda-Kleinglass, A., Michael, H., Stieglitz, T., and Scholten, J. 2021. Radium isotopes as submarine groundwater discharge (SGD) tracers: Review and recommendations. *Earth-Science Reviews*, 220:103681. doi.org/10.1016/j.earscirev.2021.103681.
- Gatto, L.W. 1976. Baseline data on the oceanography of Cook Inlet, Alaska. Report 76-25, US Army Cold Regions Research and Engineering Laboratory, Hanover, NH.
- Gu, H., Moore, W.S., Zhang, L., Du, J., and Zhang, J. 2012. Using radium isotopes to estimate the residence time and the contribution of submarine groundwater discharge (SGD) in the Changjiang effluent plume, East China Sea. *Continental Shelf Research*, 35:95-107.
- Hancock, G.J., Webster, I.T., and Stieglitz, T.C. 2006. Horizontal mixing of Great Barrier Reef waters: offshore diffusivity determined from radium isotope distribution. *Journal of Geophysical Research*, 111:C12019. doi:10.1029/2006JC003608.
- Johnson, M.A. 2021. Subtidal surface circulation in lower Cook Inlet and Kachemak Bay, Alaska. *Regional Studies in Marine Science*, 41:101609.
- Jenckes, J., Munk, L., Ibarra, D., Boutt, D., Fellman, J., and Hood, E. 2022. Hydroclimate drives seasonal riverine export across a gradient of glacierized high-latitude coastal catchments. Unpublished manuscript, Department of Geological Sciences, University of Alaska Anchorage.
- Kachemak Bay National Estuarine Research Reserve: Quarterly Report December 2017 – February 15, 2017. <https://kbaycouncil.files.wordpress.com/2017/02/kbnerr-february-2017-quarterly-report.pdf>.
- Kerouel, R., and Aminot, A. 1997. Fluorometric determination of ammonia in sea and estuarine waters by direct segmented flow analysis. *Marine Chemistry*, 57(3-4):265-275.
- Knee, K.L., and Paytan, A. 2011. Submarine Groundwater Discharge: A Source of Nutrients, Metals, and Pollutants to the Coastal Ocean. pp. 205–233 In: *Treatise on Estuarine and Coastal Science*, Vol 4. Wolanski, E., and McLusky, D.S. (eds.). Academic Press, Waltham, MA.
- Konar, B., Iken, K., Cruz-Motta, J., Benedetti-Cecchi, L., Knowlton, A., Pohle, G., Miloslavich, P., Edwards, M., Trott, T., and Kimani, E. 2010. Current patterns of macroalgal diversity and biomass in northern hemisphere rocky shores. *PLoS One*, 5:e13195.
- Kwon, E.Y., Kim, G., Primeau, F., Moore, W.S., Cho, H.-M., DeVries, T., Sarmiento, J.L., Charette, M.A., and Cho, Y.-K. 2014. Global estimate of submarine groundwater discharge based on an observationally constrained radium isotope model. *Geophysical Research Letters*, 41(23):8438-8444. doi:10.1002/2014GL061574.
- Lecher, A.L., Chien, C., and Paytan, A. 2016. Submarine groundwater discharge as a source of nutrients to the North Pacific and Arctic coastal oceans. *Marine Chemistry*, 186:167-177.
- Lecher, A.L., Mackey, K.R.M., and Paytan, A. 2017. River and submarine groundwater discharge effects on diatom phytoplankton abundance in the Gulf of Alaska. *Hydrology*, 4:61. doi:10.3390/hydrology4040061.

- Liu, Y., Jiao, J.J., Liang, W., and Luo, X. 2017. Tidal pumping-induced nutrients dynamics and biogeochemical implications in an intertidal aquifer. *Journal of Geophysical Research: Biogeosciences*, 122:3322-3342. doi.org/10.1002/2017JG004017.
- Moore, W.S., 1976. Sampling 228Ra in the deep ocean. *Deep-Sea Research and Oceanographic Abstracts* 23:647-651.
- Moore, W.S. 2000a. Ages of continental shelf waters determined from 223Ra and 224Ra. *Journal of Geophysical Research* 105:117-122. doi.org/10.1029/1999JC000289.
- Moore, W.S. 2000b. Determining coastal mixing rates using radium isotopes, *Continental Shelf Research*, 20:1993-2007.
- Moore, W. S. 2008. Fifteen years experience in measuring 224Ra and 223Ra by delayed coincidence counting, *Marine Chemistry*, 109:188-197.
- Moore, W., Beck, M., Riedel, T., van der Loeff, M.R., Dellwig, O., Shaw, T., Schnetger, B., and Brumsack, H.-J. 2011. Radium-based pore water fluxes of silica, alkalinity, manganese, doc, and uranium: A decade of studies in the German Wadden Sea. *Geochimica et Cosmochimica Acta*, 75:6535-6555.
- Murphy, J., and Riley, J.P. 1962. A modified single solution method for the determination of phosphate in natural waters. *Analytica Chimica Acta*, 27:31-36.
- Oey, L.-Y., Ezar, T., Hu, C., and Muller-Karger, F. 2007. Baroclinic tidal flows and inundation processes in Cook Inlet, Alaska: Numerical modeling and satellite observations. *Ocean Dynamics*, 57:205-221.
- Rapaglia, J., Ferrarin, C., Zaggia, L., Moore, W.S., Umgiesser, G., Garcia-Solsona, E., Garcia-Orellana, J., and Masque, P. 2010. Investigation of residence time and groundwater flux in the Venice Lagoon: comparing radium isotope and hydrodynamical models. *Journal of Environmental Radioactivity*, 101:571-581.
- Santos, I.R., Burnett, W.C., Dittmar, T., Suryaputra, I.G.N.A., and Chanton, J. 2009. Tidal pumping drives nutrient and dissolved organic matter dynamics in a Gulf of Mexico subterranean estuary. *Geochimica et Cosmochimica Acta*, 73:1325-1339.
- Santos, I.R., Chen, X., Lecher, A.L., Sawyer, A.H., Moosdorf, N., Rodellas, V., Tamborski, J., Cho, H.M., Dimova, N., Sugimoto, R., Bonaglia, S., Li, H., Hajati, M., & Li, L. 2021. Submarine groundwater discharge impacts on coastal nutrient biogeochemistry. *Nature Reviews Earth and Environment*, 2(5):307-323.
- Stabeno, P.J., Bond, N.A., Hermann, A.J., Kachel, N.B., Mordy, C.W., and Overland, J.E. 2004. Meteorology and oceanography of the Northern Gulf of Alaska. *Continental Shelf Research*, 24(7-8):859-897.
- Sun, Y., and Torgersen, T. 1998. The effects of water content and mn-fiber surface conditions on 224Ra measurement by 220Rn emanation. *Marine Chemistry*, 62:299-306.
- Wang, X., Li, H., Jiao, J.J., Barry, D.A., Li, L., Luo, X., Wanbg, C., Wan, L., Wang, X., Jiang, X., Ma, Q., and Qu, W. 2015. Submarine fresh groundwater discharge into Laizhou Bay comparable to the Yellow River flux. *Scientific Reports*, 5(1):1-7.



The Department of the Interior Mission

As the Nation's principal conservation agency, the Department of the Interior has responsibility for most of our nationally owned public lands and natural resources. This includes fostering the sound use of our land and water resources, protecting our fish, wildlife and biological diversity; preserving the environmental and cultural values of our national parks and historical places; and providing for the enjoyment of life through outdoor recreation. The Department assesses our energy and mineral resources and works to ensure that their development is in the best interests of all our people by encouraging stewardship and citizen participation in their care. The Department also has a major responsibility for American Indian reservation communities and for people who live in island communities.



The Bureau of Ocean Energy Management

The Bureau of Ocean Energy Management (BOEM) works to manage the exploration and development of the nation's offshore resources in a way that appropriately balances economic development, energy independence, and environmental protection through oil and gas leases, renewable energy development and environmental reviews and studies.